Renewable and Sustainable Energy Reviews 82 (2018) 2440–2454

Contents lists available at ScienceDirect

Renewable and Sustainable Energy Reviews

journal homepage: www.elsevier.com/locate/rser

Current status of water electrolysis for energy storage, grid balancing and sector coupling via power-to-gas and power-to-liquids: A review

Alexander Buttler[a,*], Hartmut Spliethoff[a,b]

[a] TU München, Lehrstuhl für Energiesysteme, Boltzmannstr. 15, 85748 Garching b. München, Germany
[b] ZAE Bayern, Walther-Meißner-Str. 6, 85748 Garching b. München, Germany

ARTICLE INFO

Keywords:
Alkaline electrolysis
PEM electrolysis
SOEC
Energy storage
Market survey
Investment costs
System performance

ABSTRACT

Water electrolysis has the potential to become a key element in coupling the electricity, mobility, heating and chemical sector via Power-to-Liquids (PtL) or Power-to-Gas (PtG) in a future sustainable energy system. Based on an extensive market survey, discussions with manufacturers, project reports and literature, an overview of the current status of alkaline, PEM and solid oxide electrolysis on the way to large-scale flexible energy storage is presented. These main water electrolysis technologies were compared in terms of available capacity, nominal and part-load performance, flexibility (load range, load gradients, start-up time, stand-by losses) lifetime and investment costs. This review provides a basis of the parameters required and the necessary understanding of electrolysis fundamentals and technologies for a techno-economic analysis of water electrolysis-based concepts and an evaluation of PtG and PtL in energy system studies.

1. Introduction

Power-to-Gas (PtG) and Power-to-Liquids (PtL) are often discussed as important elements in a future renewable energy system (e.g. [1–3]). The conversion of electricity via water electrolysis and optionally subsequent synthesis together with CO or CO_2 into a gaseous or liquid energy carrier enables a coupling of the electricity, chemical, mobility and heating sectors. This opens up enormous storage or absorption capacities for excess energy with high electricity generation from renewable energies in excess of demand. It also supports the integration of fluctuating renewables like wind and solar power in the energy system, including the provision of balancing power. By substituting fossil fuels, this can help to reduce greenhouse gas emissions in the mobility or chemical sectors. The future demand for Power-to-Liquids and Power-to-Gas energy storage represents an emerging market for electrolysis systems. Operating strategies such as the absorption of excess energy at limited operating times per year, providing grid services or arbitrage trading (exploitation of highly fluctuating electricity prices) are possible, which also could be combined [4]. This poses new requirements regarding efficiency, flexibility, part-load and stand-by performance, electrolyser capacity (multi MW to GW plants) and capital costs, depending on the specific application and operating strategies.

There have been several excellent reviews on electrolysis technologies in general [4–8] as well as on AEL (alkaline electrolysis) [9,10], PEMEL (proton exchange membrane electrolysis) [11], and SOEL (solid oxide electrolysis) [12–14]. Moreover, the FCH JU (Fuel Cells and Hydrogen Joint Undertaking) under the EU's funding programme Horizon 2020 has implemented key performance indicators (KPIs) for flexible water electrolysis as a target and for monitoring their multi annual work programme (Table 1) [15].

The scope of this review is on commercial technologies and research related to flexible electrolysis operation and performance relevant for PtG and PtL applications. It provides an overview of the current status of water electrolysis on the way to large-scale flexible energy storage applications. After dealing with the fundamentals of water electrolysis, the major electrolysis technologies (AEL, PEMEL, SOEL) are compared with regard to the available capacity, nominal and part-load performance, flexibility (load range, load gradients, start-up time, stand-by losses) lifetime and investment costs. This comparison is based on the above-mentioned literature reviews, discussions with manufacturers, project reports and an extensive market survey of electrolysis suppliers.

2. Fundamentals of water electrolysis

The overall reaction of electrochemical splitting of water into hydrogen and oxygen by supplying electrical (and thermal) energy is given by:

$$H_2O \xrightarrow[\text{Electrolysis}]{} H_2 + \frac{1}{2}O_2 \quad (2.1)$$

* Corresponding author.
E-mail address: buttler@es.mw.tum.de (A. Buttler).

http://dx.doi.org/10.1016/j.rser.2017.09.003
Received 26 February 2017; Accepted 3 September 2017
Available online 09 September 2017
1364-0321/

Table 1
State-of-the-art (SoA) and future targets of key performance indicators (KPIs) given by FCH JU [15] for hydrogen production from renewable electricity for energy storage and grid balancing (KPI 1, 2 and 3 are extended by own calculations marked in italics, conversion of values of KPI 2 and 3 are based on energy consumption specified in KPI 1).

		SoA in 2012	2017	2020	2023
KPI 1	Energy consumption @ rated power	57–60 kWh/kg @100 kg/d *5.1–5.4 kWh/Nm³*	55 kWh/kg @500 kg/d *4.9 kWh/Nm³*	52 kWh/kg @1000 + kg/d *4.7 kWh/Nm³*	50 kWh/kg @1000+ kg/d *4.5 kWh/Nm³*
KPI 2	CAPEX @ rated power including auxiliary equipment and commissioning	8 M€/(t/d) *3400 €/kW$_{el}$*	3.7 M€/(t/d) *1600 €/kW$_{el}$*	2.0 M€/(t/d) *900 €/kW$_{el}$*	1.5 M€/(t/d) *700 €/kW$_{el}$*
KPI 3	Efficiency degradation @ rated power and 8000 h operation / year	2–4%/year *5.4–10.7 μV/h*	2%/year *5.2 μV/h*	1.5%/year *3.7 μV/h*	< 1%/year *< 2.3 μV/h*
KPI 4	Flexibility with a degradation < 2% per year (refer to KPI 3)	5–100% of nominal power	5–150% of nominal power	0–200% of nominal power	0–300% of nominal power
KPI 5	Hot start from min to max power (refer to KPI 4) Cold start	1 min 5 min	10 s 2 min	2 s 30 s	< 1 s 10 s

KPI 4 and KPI 5 shall be considered as optional targets to be fulfilled according to the profitability of the services brought to the grid thanks to the addition of flexibility and (or) reactivity (considering also potential degradation of the efficiency and lifetime duration).
"H2 Production … @ rated power" – corrected for 30 bar hydrogen output pressure.

The volumetric co-production of oxygen corresponds to half the production of hydrogen. The heat of reaction gives the overall energy demand of reaction ΔH, which can be partly supplied by heat (ΔQ) while another part (change in Gibbs energy ΔG), has to be supplied electrically:

$$\Delta H = \Delta G + \Delta Q \tag{2.2}$$

As shown in Fig. 1, the overall energy demand ΔH varies only slightly with temperature (between 283.5 and 291.6 kJ/mol H_2 in the illustrated temperature range of 0–1000 °C). However, the share of possible heat integration ΔQ rises with temperature, reducing the minimum electrical demand ΔG. Beside improved kinetics, the possible high heat utilisation of internal losses is a major motivation of high temperature electrolysis operated at 700–900 °C. Moreover, part of the heat demand corresponding to the latent heat of vapourisation is supplied by feeding water vapour instead of liquid water, as it is the case for low temperature electrolysis (AEL, PEMEL).

The theoretical minimum cell voltage of electrolysis operation, the reversible cell voltage U_{rev}, is characterised by a necessary external thermal supply of the whole heat demand ΔQ. It is directly proportional to the change in Gibbs free energy ΔG:

$$U_{rev} = \frac{\Delta G}{z\mathrm{F}} \tag{2.3}$$

where z is the number of electrons transferred per reaction (z = 2) and F represents the Faraday's constant (96 485 C/mol). U_{rev} decreases with rising temperature. It lies in the range of 1.25–0.91 V in the temperature range of 0–1000 °C (see Fig. 1).

The thermoneutral cell voltage gives the minimum voltage for electrolysis to take place in an ideal cell without heat integration (but in case of high temperature electrolysis, water is supplied as steam, which means that it had to be evaporated externally):

$$U_{tn} = \frac{\Delta H}{z\mathrm{F}} \tag{2.4}$$

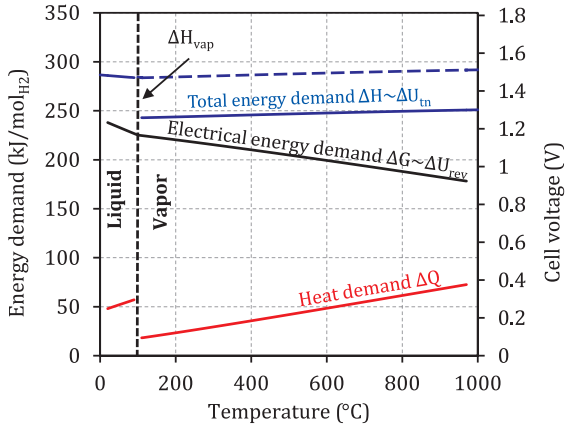

Fig. 1. Total (ΔH), thermal (Q) and electrical (ΔG) energy demand of an ideal electrolysis process as function of the temperature.

This means that the overall energy demand of the electrolysis reaction (including heat) is supplied electrically. The thermoneutral cell voltage is approx. 1.47–1.48 V (284–286 kJ/mol_{H2}) feeding liquid water below 100 °C while it reduces to 1.26–1.29 V (243–249 kJ/mol_{H2}) in the temperature range of 100–1000 °C if steam is supplied (see Fig. 1). This means that the minimum electrical energy consumption of steam electrolysis compared to liquid water electrolysis can be reduced by the heat of evaporation of 41 kJ/mol at ambient pressure. The total energy consumption including evaporation of the water is almost constant from 0 to 1000 °C. However, steam electrolysis offers the possibility to replace high valuable electrical energy in the order of 0.5 kWh/Nm^3 (41 kJ/mol) of hydrogen by low temperature heat for water evaporation. In a real electrolyser the cell voltage for thermoneutral operation is slightly higher than U_{tn} due to heat losses (non-adiabatic operation) and thermodynamic irreversibilities [5].

Thermoneutral voltage represents the standard operation mode of high temperature electrolyser. The cell is operated at constant temperature as internal heat production by irreversibilities is equalised by heat consumption of the electrolysis reaction. Low temperature electrolysers (AEL, PEMEL) are operated above the thermoneutral voltage due to high internal losses or overvoltages. This results in a heating of the electrolysis cells requiring external cooling of the module. The cell voltage can be expressed as the sum of the reversible cell voltage U_{rev} and the overvoltages caused by ohmic resistance U_{ohm}, limitations in electrode kinetics (activation overvoltages U_{act}) and mass transport (concentration overvoltages U_{con}) [16]:

$$U = U_{rev} + U_{ohm} + U_{act} + U_{con} \tag{2.5}$$

The dependency between cell voltage and current or current density respectively is shown exemplary in Fig. 2. The current-voltage (I-U) relationship characterises the electrochemical behaviour of an electrolysis cell. The current density is approximately proportional to the hydrogen production rate according to Faraday's law. However, Faraday's law of an ideal electrolysis cell has to be extended by the Faraday efficiency η_F (or current efficiency) which is defined as the ratio of actual to theoretical hydrogen production rate. This deviation is caused by parasitic current losses along the gas ducts and cross permeation of product gases. Cross permeation of product gases increases with temperature and pressure and this negative effect is higher at low current densities due to lower gas production [17–21]. Parasitic current losses are especially relevant for AEL. The parasitic currents increase at lower

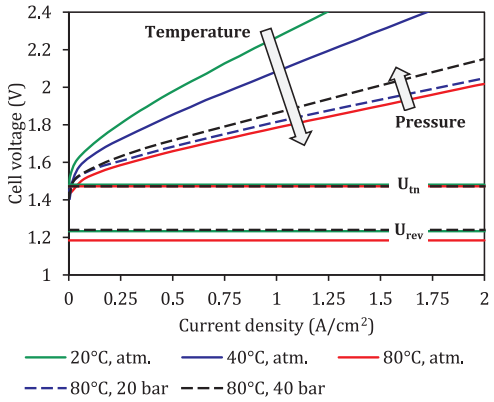

Fig. 2. Influence of temperature and pressure on the characteristic I-U-curve of a PEM electrolysis cell (experimental data from [25], U_{tn} and U_{rev} based on own calculations).

electric resistance caused by lower current densities and higher temperature [16,22]. At nominal current density, the Faraday efficiency of AEL, PEMEL and SOEL is reported to be close to 100% (98–99.9%) [9,16,17,21–24]. A strong decrease in Faraday efficiency is observed below a current density of 50–100 mA/cm^2 for AEL [16,22]. Grigoriev et al. report a decrease of the Faraday efficiency of a PEM electrolyser from nearly 100% at pressures up to 20 bar to 90% at a pressure of 130 bar [17].

For the prevailing bipolar modules (properties of bipolar and monopolar modules are very well discussed by Ursua et al. [5]) with a number of n_c electrolysis cells electrically connected in series and operated at a current I in A, the total hydrogen production rate in Nm^3/h is given as follows:

$$\dot{V}_{H_2} = \eta_F \frac{n_c I}{2F} \times \left[22.414 \bullet 3.6 \frac{Nm^3/h}{mol/s} \right] \tag{2.6}$$

The efficiency of an electrolyser is defined as:

$$\eta_{HHV} = \frac{\dot{V}_{H_2} HHV_{H2}}{P_{el}} \tag{2.7}$$

where $\dot{V}_{H_2}$ is the volume flow of hydrogen in Nm^3/h, HHV_{H2} the higher heating value of hydrogen (3.54 kW h/Nm^3) and P_{el} the electric energy consumption in kW. While the current (or current density respectively) is approximately proportional to the theoretical hydrogen production rate (as long as Faraday efficiency is close to 100% which is not the case at low current densities as discussed before), the cell voltage U_c given in V is inversely proportional to the efficiency:

$$\eta_{HHV} = \frac{\eta_F \frac{n_c I}{2F} HHV_{H2}}{n_c U_c I} = \frac{1.48\ V}{U_c} \bullet \eta_F \tag{2.8}$$

The efficiency of low temperature electrolyser is often given based on the higher heating value as the higher heating value corresponds to the enthalpy of reaction at standard conditions from liquid water to gaseous hydrogen [7]. However, for the evaluation of an overall process chain, the partial efficiencies of the process steps and fuel prices are usually referred to the lower heating value. Therefore, it is expedient to use the electrolyser efficiency referred to the lower heating value LHV_{H2} (3.00 kW h/Nm^3):

$$\eta_{LHV} = \frac{\dot{V}_{H_2} LHV_{H2}}{P_{el}} = \frac{3.00}{3.54} \bullet \eta_{HHV} = \frac{1.25V}{U_c} \bullet \eta_F \tag{2.9}$$

Unless otherwise indicated, all efficiencies given within this paper are related to the lower heating value. Beside efficiency, the specific energy consumption for the production of 1 Nm^3 (or 1 kg) of hydrogen is often specified, which is proportional to the cell voltage:

$$E_s = \frac{LHV_{H2}}{\eta_{LHV}} = \frac{2.4}{\eta_F} \bullet U_c/V \tag{2.10}$$

The efficiency of an electrolyser decreases (or the overpotentials increase respectively):

- with rising current density
- with decreasing temperature
- slightly with increasing pressure

The operating temperature has a strong influence on performance but it is limited by degradation issues of the electrolysis cells and material restrictions. Low temperature electrolysers are operated at temperatures of 60–90 °C while SOEL is operated at 700–900 °C. Typical operating conditions regarding pressure and current density of AEL, PEMEL and SOEL are discussed in Sections 5.1 and 5.2. The selection of the nominal current density of a system represents a weighting up of operating and capital costs as higher current densities result in:

- increased hydrogen production per cell area corresponding to reduced specific capital costs per Nm^3 of hydrogen production
- in a decrease in performance corresponding to an increase in operational costs
- an increase in the deactivation rate due to higher overpotentials.

Based on the nominal current density, part-load operation corresponds to a reduced current density and a higher efficiency. This means that each electrolyser can reach very high efficiencies in part-load. As a result, the nominal specific energy consumption in kW h per Nm^3 of hydrogen often given by manufacturer is not meaningful without specifying the nominal current density. Therefore, the characteristic I-U-curve of an electrolysis cell is a better measure for electrolysis performance (also in part-load) and a survey of I-U-curves of AEL, PEMEL and SOEL will be given in Section 5.2.

3. Water electrolysis technologies

Water electrolysis technologies can be classified according to the applied electrolyte, which separates the two half reactions at the anode (oxygen evolution reaction) and cathode (hydrogen evolution reaction) of the electrolyser [7]. The main water electrolysis technologies are Alkaline Electrolysis (AEL), Polymer Electrolyte Membrane Electrolysis (PEMEL) and Solid Oxide Electrolysis (SOEL). The principle layout, reactions and relating properties of AEL, PEMEL and SOEL are discussed in the following.

3.1. Alkaline electrolysis (AEL)

Alkaline electrolysis represents a mature technology, which has been applied for large-scale hydrogen production in the MW-scale already in the beginning of the 20th century [26]. The principle layout of an alkaline electrolyser is shown in Fig. 3. The electrodes are immersed in a liquid electrolyte separated by a diaphragm. The electrolyte is usually a 25–30% aqueous KOH-solution. It is circulated for the removal of product gas bubbles and heat either by pumps or by natural circulation due to temperature gradients and buoyancy of the gas bubbles. The electrolyte is stored in two separated drums for each product gas (O_2 and H_2) which serve also as gas-liquid-separator. The product gas quality after drying is typically in the range of 99.5–99.9% for H_2 and 99–99.8% for O_2 [27–35] which can be increased to above 99.999% by catalytic gas purification (deoxidiser) [27,28,34,35]. The partial reaction at the electrodes is given by:

$$2H_2O + 2e^- \rightarrow H_2 + 2OH^- \text{ Cathode} \tag{3.1.1}$$

$$2OH^- \rightarrow \frac{1}{2}O_2 + H_2O + 2e^- \text{ Anode} \tag{3.1.2}$$

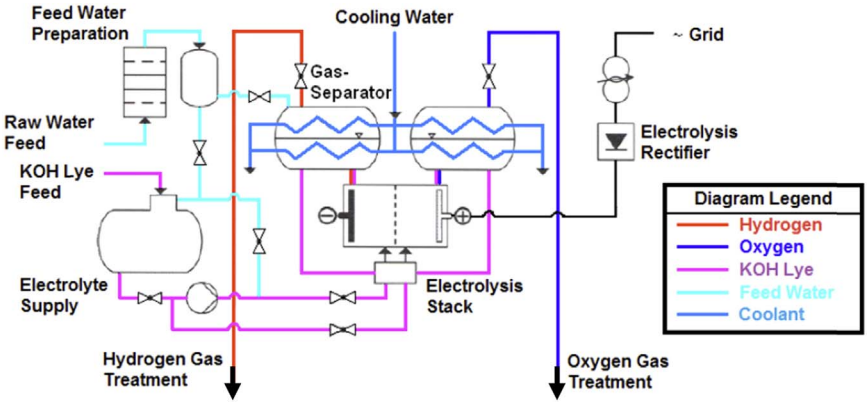

Fig. 3. Layout of an alkaline electrolysis system (modified from [35]).

As seen, water is consumed on the cathode side while water is produced on the anode side. As a result, the lye streams of both sides have to be mixed before entering the electrolyser to prevent a respective dilution or concentration of the electrolyte streams. This results in a contamination of product gases due to the electrolyte streams carrying dissolved gases, as the separators can only remove the gas bubbles [19,36]. A critical contamination (flammable mixture) in part-load has to be avoided by a proper control of the lye circulation, which is automatically the case for natural circulation [19,37].

3.2. PEM electrolysis (PEMEL)

Polymer Electrolyte Membrane or Proton Exchange Membrane (PEM) electrolysis, sometimes also referred as Solid Polymer Electrolysis (SPE), was introduced by General Electrics in the 1960s [11]. The basic layout of a PEM electrolyser is shown in Fig. 4. A proton exchange membrane (Nafion® membrane in most cases) separates the two half-cells, and the electrodes are usually directly mounted on the membrane forming the MEA (membrane electrode assembly). The corrosive acidic regime provided by the proton exchange membrane requires the use of noble metal catalysts like iridium for the anode and platinum for the cathode [11]. Water is supplied at the anode (partly transported to the cathode side due to the electroosmotic effect) and the following partial reactions take place:

$$2H^+ + 2e^- \rightarrow H_2 \text{ Cathode} \quad (3.2.1)$$

$$H_2O \rightarrow \frac{1}{2}O_2 + 2H^+ + 2e^- \text{Anode} \quad (3.2.2)$$

The polymer electrolyte membrane features a very low cross-permeation, yielding hydrogen with a higher purity than AEL of typically greater than 99.99% H_2 after hydrogen drying [5,38]. PEM electrolysis features a compact module design due to the solid electrolyte and high current density operation compared to AEL (see Section 5.1). This supports the high-pressure operation of PEM electrolysis (see Section 5.2). The structural properties of the solid electrolyte also allow a high differential pressure between the hydrogen and the oxygen side (currently, stacks operated at up to 350 bar differential pressure are reported [39,40]).

3.3. Solid oxide electrolysis (SOEL)

The development of solid oxide electrolysis was begun in the USA in the 1970s by General Electric and Brookhaven National Laboratory, followed by Dornier in Germany [7]. In recent years, SOEL has attracted increasing interest due to the progress in solid-oxide fuel cells and the motivation of carbon-neutral energy scenarios [12]. SOEL operates at temperatures of 700–900 °C. High temperature operation results in higher efficiencies than AEL or PEMEL but implies a remarkable challenge for material stability. The efficiency advantages result from improved kinetics, thermodynamics favouring internal heat utilisation at higher temperature and the conversion of steam, as discussed earlier. A simplified process layout of a SOEL system is shown in Fig. 5. The reactions at the electrodes are:

$$H_2O + 2e^- \rightarrow H_2 + O^{2-} \text{ Cathode} \quad (3.3.1)$$

$$O^{2-} \rightarrow \frac{1}{2}O_2 + 2e^- \text{Anode} \quad (3.3.2)$$

The feed water or steam is pre-heated in a recuperator against the hot product streams leaving the stack. Additionally, low temperature heat has to be integrated or electrical heating is required to account for the heat of evaporation. The stack consists typically of planar cells electrically connected in series. Steam, and recycled hydrogen to maintain reducing conditions, are supplied to the cathode and partly converted to hydrogen. The reactant utilisation increases with current

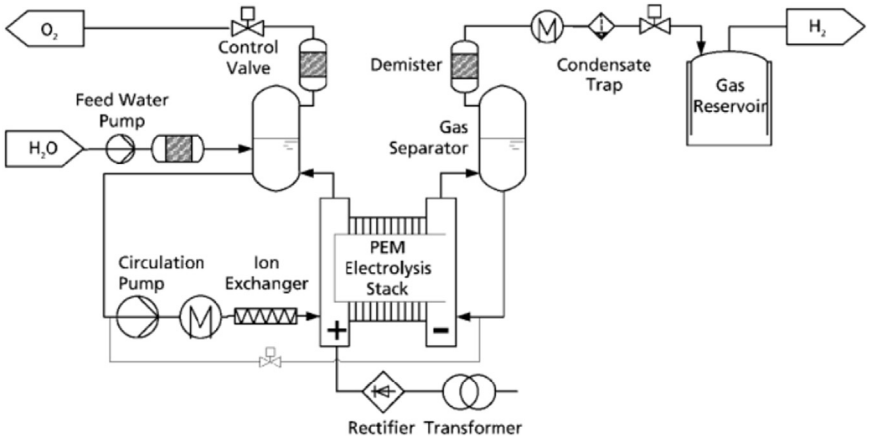

Fig. 4. Layout of a PEM electrolysis system [25].

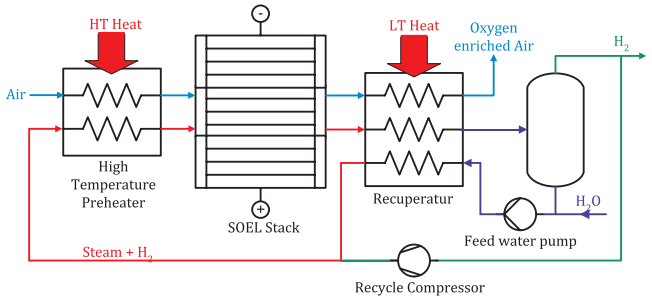

Fig. 5. Simplified layout of a SOEL system including the necessary high-temperature (HT) and low-temperature (LT) heat integration (often achieved by electrical heaters).

density (at constant feed flow). Experimental reactant utilisation typically lies in the range of 40–80% [24,41–45]. Optionally air can be used at the anode as sweep stream for the removal of product oxygen despite of the efficiency penalty due to the critical handling of high-temperature pure oxygen [46]. The mixture of steam and hydrogen is separated by cooling and condensing of the water. Due to exergetic losses of the heat exchanger and the difference in heat capacity of the make-up steam and the SOEL product gas, the steam has to be further superheated to reach the SOEL inlet temperature of 700–1000 °C. The high temperature heat is either supplied by an external heat source or by an electrical heater [47]. Heat integration with subsequent exothermal synthesis processes (e.g. methanol, DME, substitute natural gas or FT-Diesel) represents an interesting application as shown in [43,48–51].

Current electrolysis cells are often operated below thermoneutral voltage in endothermic mode (see Section 5.1) due to the current density limitation below 1 A/cm^2 for degradation reasons (see Section 5.5). This requires additional preheating of the feed gas to hold the temperature of the system constant [52]. Additionally, high-temperature heat integration is possible with the aim of reducing the electrical demand. However, this increases the specific cell area, which is currently not economically reasonable [53].

An interesting feature of SOEL is the ability of co-electrolysis of CO_2 and steam to produce a syngas containing H_2 and CO for the synthesis of fuels (e.g. [42,45,48,51,54–58]). Another interesting application of SOEL represents reversible operation increasing the capacity utilisation. The possibility of flexible operation between fuel cell and electrolysis mode was recently investigated experimentally by Fuel Cell Energy [59], Haldor Topsoe [60] and Sunfire [61]. To summarise, SOEL offers several interesting features with a high potential for PtG and PtL applications. However, SOEL is still at the research stage based on single-cell or short-stack tests, although the company Sunfire does offer commercial reversible SOEL systems and has demonstrated a small-scale FT-diesel production (1 bbl/day) [61,62].

4. Market survey of electrolysis technologies

The electrolysis market is very dynamic with several fusions and acquisitions in recent years (e.g. McPhy acquired Piel (IT) and Hytec Enertrag (DE) in 2013, Areva H2Gen, resulting from the fusion of Areva Helion and CETH2 in 2014, Hitachi Zosen Inova (CH) acquired ETOGAS (DE) in 2016, NEL Hydrogen (NO) aquired Proton OnSite (US) in 2017, Accagen (CH) became EnerBlue in 2013). In this context, the companies H2Nitidor [63] (using Voltiana technology from Casale Chemicals) and Avalance [64] in our electrolysis database could not be found in a recent internet search.

An overview of the researched manufacturers of medium to large-scale electrolysis systems is given in Table 2 (only the largest stack series are mentioned). Manufacturers of laboratory-scale electrolysers (e.g. Schmidlin, Claind) are not considered. In summary, 20 manufacturers of alkaline electrolysis (Casale Chemicals [65] is excluded in Table 2 as no current information was available) and 12 manufacturers of PEM electrolysis could be identified. Additionally manufacturers of chloralkali electrolysis are about to enter the water electrolysis market like Thyssen Krupp (DE) [66] and Asahi Kasai (JP) [67].

SOEL is in a pre-commercial and fundamental research stage although Sunfire is already offering systems of 150 kW in a 20 ft or 40 ft container. Other companies investigating SOEL are Haldor Topsoe (in cooperation with Riso DTU) [12], Cermatec (in cooperation with the Idaho National Laboratory) [68], FuelCell Energy [59] and Toshiba [24].

Beside the main technologies, one commercial supplier of anion exchange membrane (AEM) electrolysis was identified though it will not be treated in more detail within this review. Acta (IT) offers small-scale stacks with a capacity of 1 Nm^3/h at 30 bar [69].

5. Comparison of technologies

5.1. Nominal and part-load performance

Electrolysers feature an increase in performance in part-load as discussed before. Therefore, the efficiency of an electrolyser including part-load operation is best characterised by its I-U-curve (cell voltage vs. current density). After discussing the rated specific energy consumption of commercial electrolysers, a survey of exemplary I-U-curves for AEL, PEMEL and SOEL from literature is given in the following.

Rated efficiency and specific energy consumption of commercial electrolysis stacks are in the range of 63–71%$_{LHV}$ and 4.2–4.8 kW h/Nm^3 for AEL and 60–68%$_{LHV}$ and 4.4–5.0 kW h/Nm^3 for PEMEL (based on Table 2). Given specific energy consumptions of electrolysis systems (including rectifier and utilities, excluding external compression) are in the range of 5.0–5.9 kW h/Nm^3 (η_{LHV} = 51–60%) for AEL and 5.0–6.5 kW h/Nm^3 (η_{LHV} = 46–60%) for PEMEL. The additional consumption of utilities and losses by rectification lies typically in the range of 0.4–0.8 kW h/Nm^3 [89,97–100]. A reduced performance at lower capacity is observed for electrolysis systems below a hydrogen production rate of approx. 100 Nm^3/h (0.5 MW), mainly due to the decreasing efficiency of the utilities [7]. However, the rated specific energy consumption is only meaningful in combination with the current density. Additionally, the decrease in performance over lifetime must be taken into account, as discussed in Section 5.5.

Characteristic I-U-curves of AEL are summarised in Fig. 6. Commercial electrolysers reach current densities up to 0.45 A/cm^2 [35,70,101], corresponding to a theoretical specific hydrogen production rate of 1.9 Nm^3 per m^3 of cell area. The cell voltage at a current density of 0.4 A/cm^2 varies between 1.7–2.1 V, corresponding to a specific energy stack consumption of 4–5 kWh/Nm^3 (η_{LHV} = 60–75%). Exceptions are the results from GHW (Gesellschaft für Hochleistungselektrolyseure, now part of NEL Hydrogen) [19] with current densities up to 1 A/cm^2, which are not applied in commercial operation however. Another exception is the cell performance presented by Wasserelektrolyse Hydrotechnik [102] with very high overpotentials and a low current density of 0.25 A/cm^2 only. This is due to the use of a non-activated anode for reliable operation under harsh conditions in remote areas.

In part-load operation, the stack-efficiency based on LHV is increased up to 73–86% (E_s = 3.5–4.1 kWh/Nm^3) at 0.1 A/cm^2 (25% based on nominal current density of 0.4 A/cm^2). However, decreasing Faraday efficiency and relatively increasing consumption of utilities have to be taken into account for overall system performance.

Overall efficiency of AEL systems including compression are stated to be approx. 50%, based on HHV (η_{LHV} = 42%) in the HARI project (36 kW electrolyser, compression to maximum 137 bar) [103] and Res2H2 project (25 kW electrolyser, compression to maximum 220 bar) [104]. However, a poor rectifier efficiency of 72–89% is reported in the HARI project. Within the “Power-to-Gas” project, a total efficiency of 53% based on LHV is reached at full load operation (10 bar hydrogen pressure, including all auxiliaries), which increase slightly to 55% at a

Table 2
Overview of commercial electrolysis systems (not exhaustive, only the largest systems from each supplier are listed).

Manufacturer (location)	Series	H_2 rate, Nm^3/h[a]	Nominal power, MW[a]	Max. pressure, bar	Specific energy consumption[a,b], kWh/Nm^3	η_{LHV}[a,b,c], %	Load flexibility (%)	Ref.
Alkaline electrolysis (AEL)								
ELB (DE)	LURGI SE[d]	1400	6.0	30	4.3–4.65	65–70	25–100	[28,70]
Suzhou Jingli (CN)	DQ 1000	1000	4.7	16	4.7	64	10–110	[32]
Verde (US)	Verde − 1000	1000	4.5	30	4.2	79	n.a.	[30]
IHT (CH)	S − 556[d]	760	3.5	32	4.3–4.65	65–70	25–100	[71]
PERIC[e] (CN)	ZDQ − 600	600	2.8	15	4.6	65	n.a.	[29,34]
NEL Hydrogen[f] (NO)	NEL A485	485	2.1	atm.[g]	3.8–4.4	68	20–100	[72]
ELB(DE)	ELB ND4	480	2.0	atm.[g]	4.3–4.6	71	25–100	[28,70]
Teledyne[h] (US)	NH − 450	450	2.7	10	(5.9[i])	(51)	17–100	[73,74]
McPhy[j] (FR)	McLyzer	400	2.0	atm.[g]	n.a.	n.a.	n.a.	[75]
Tianjin Mainland (CN)	FDQ − 400/3.0	400	1.76	30	< 4.4	68	n.a.	[76]
Ener Blue (CH)	L-size	375	1.6	60	4.3	70	n.a.	[77]
ELB(DE)	BAMAG S300E	330	1.5	atm.[g]	4.7	64	25–100	[28,70]
Uralhimmasch (RU)	BEU − 250	250	n.a.	10	n.a.	n.a.	n.a.	[78]
HT-Hydrotechnik (DE)	EV 150	220	1.1	atm.[g]	(5.3)	(57)	20–100	[34]
Uralhimmasch (RU)	FV − 200	200	n.a.	atm.[g]	n.a.	n.a.	n.a.	[78]
McPhy [j] (FR)	McLyzer	100	0.5	45	n.a.	n.a.	n.a.	[75]
Idroenergy (IT)	Model 120	80	0.4	6	(5.6)	(54)	n.a.	[79]
ETOGAS (DE)		62.5[k]	0.3	15	4.8	63	10–110	[33]
Green Hydrogen (DK)	HyProvide A60	60	0.25	30	4.2	72	15–100	[80]
ErreDue[l] (IT)	G256[m]	21	0.11	30	(5.4)	(56)	20–100	[27,81]
Hydrogenics[n](CA)	HySTAT-100–10[o]	15	0.08	10(25)	(5.2)	(58)	40–100	[82,83]
Sagim (FR)	M 5000	5	0.03	7	(5)	(60)	n.a.	[84]
Linde AG (DE)	HYDROSS	n.a.[p]	n.a.	25	n.a.	n.a.	25–100	[85]
PEM electrolysis (PEMEL)			MW					
Giner Inc. (US)	Allagash[q]	400	2	40	5	60	n.a.	[86]
Hydrogenics[n](CA)	HyLYZER − 3000[r]	300	1.5	30	(5–5.4)	(56–60)	1–100	[83]
Siemens (DE)	SILYZER 200	225	1.25	35	(5.1–5.4)	(56–69)	0–160	[87]
ITM Power (GB)		127[s]	0.7	20–80	(5.5)	(54)	n.a.	[88]
Proton OnSite (US)	M400[t]	50	0.25	30	5	60	0–100	[38]
AREVA H2Gen[u] (FR)	E120[v]	30	0.13	35	4.4	68	10–150	[89,90]
H-TEC (DE)	ELS450	14.1	0.06	30/50	4.5	67	n.a.	[91]
Treadwell Corp. (US)		10.2	n.a.	76	n.a.	n.a.	n.a.	[92]
Angstrom Advanced (US)	HGH170000	10	0.06	4	(5.8)	(52)	n.a.	[93]
Kobelco Eco-Solutions (JP)	SH/SL60D[w]	10	0.06	4–8	(5.5–6.5)	(46–55)	0–100	[94]
Sylatech (DE)	HE 32	2	0.01	30	4.9	61	n.a.	[95]
GreenHydrogen[x] (DK)	HyProvide P1	1	0.01	50	(5.5)	(55)	n.a.	[80]
Solid oxide electrolysis (SOEL)			**kW**					
Sunfire (DE)	RSOC	~0.6	2.2[y]	10	(3.7)	(96)	−100 to 100[z]	[96]

[a] Entries in column 3, 4, 6 and 7 are partly our own calculations based on other relevant columns.
[b] Specific energy consumption of the stack, values for the overall system given by manufacturers are indicated in brackets.
[c] Efficiency calculation based on LHV of hydrogen (3 kW h/Nm^3), efficiency based on HHV of hydrogen (3.54 kW h/Nm^3) is 18% higher.
[d] ELB and IHT are based on the same technology.
[e] Electrolysis technology of PERIC distributed by Wasserelekctrolyse Hydrotechnik in Germany.
[f] NEL Hydrogen acquired GHW (DE), H2Logic (DK), Proton Onsite (US) and Rotolyzer (NO).
[g] "atm." means close to atmospheric pressure (20–40 mbar).
[h] Modules are supplied by Next Hydrogen Corporation (CA).
[i] 5.9 kWh/Nm^3 at nominal production rate of 450 Nm^3/h, 5.1 kWh/Nm^3 at 225 Nm^3/h.
[j] McPhy acquired Piel (IT) and Hytec Enertrag (DE) in 2013.
[k] ETOGAS offers systems with a hydrogen capacity of 250 Nm^3/h, 1.2 MW, consisting of 4 stacks.
[l] Modules of ErreDue are also sold by Pure Energy Centre (GB).
[m] ErreDue offers systems (G256) up to a hydrogen capacity of 171 Nm^3/h, 0.9 MW, consisting of 8 stacks, a doubling of the current stack capacity is in development.
[n] Hydrogenics acquired Stuart Energy (CA) which acquired Vandenborre Hydrogen Systems (BE) and Elwatec (DE).
[o] Hydrogencis offers the skid-mounted system HySTAT-100-10 with a hydrogen capacity of 100 Nm^3/h, 0.5 MW, consisting of 6 cell stacks.
[p] HYDROSS is offered with a hydrogen capacity up to 250 Nm^3/h, number of cell stack was not available.
[q] Giner is developing a stack with a rated hydrogen capacity of about 1100 Nm^3/h at 15.5 bar (Kennebec stack).
[r] Hydrogencis offers HyLYZER-3000-30 as an indoor installation with a hydrogen capacity of 3000 Nm^3/h, 15 MW, consisting of 10 cell stacks.
[s] ITM Power offers a platform with a capacity of 1365 kg/day (630 Nm^3/h), 3.5 MW, consisting of 5 stacks.
[t] Proton Onsite offers modular, skid-based systems up to 400 Nm^3/h (M400), 3 MW consisting of 8 cell stacks.
[u] AREVA H2Gen results from the fusion of AREVA Helion (FR) and CETH2 (FR) in 2014.
[v] AREVA H2Gen offers skid-mounted systems up to 120 Nm^3/h (E120), 0.6 MW, consisting of four stacks.
[w] Kobelco Eco-Solutions offers skid-mounted systems up to 60 Nm^3/h (SH/SL60D), 0.3 MW, consisting of six stacks.
[x] GreenHydrogen ApS and EWII Fuel Cells A/S (former IRD) have entered into a long-term partnership for the commercialisation of EWII Fuel Cells PEM electrolyser ELZE1050.
[y] Modules with a rated electrical power of 150 kW (40 Nm^3) are offered by Sunfire.
[z] Reversible operation of SOC in electrolysis and fuel cell mode possible, idle mode close to operation temperature possible.

minimum load of 40% of full load [100]. The efficiency of the rectifier increases from 94.6% at full load to above 98% at minimum load.

An overview of characteristic I-U-curves of PEMEL is given in Fig. 7. PEMEL is typically operated at higher current densities of presently approx. 1–2 A/cm^2 [90,91,97,105,106] although laboratory tests up to 20 A/cm^2 are reported [107]. A current density of 2 A/cm^2 corresponds to a theoretical specific hydrogen production rate of up to 8.4 Nm^3 per m^2 of cell area, which is over four times higher than for AEL. The cell voltages at a nominal current density of 2 A/cm^2 are in the range of 1.65–2.5 V (4.0–6.0 kW h/Nm^3, η_{LHV} = 50–76%), which is in the same

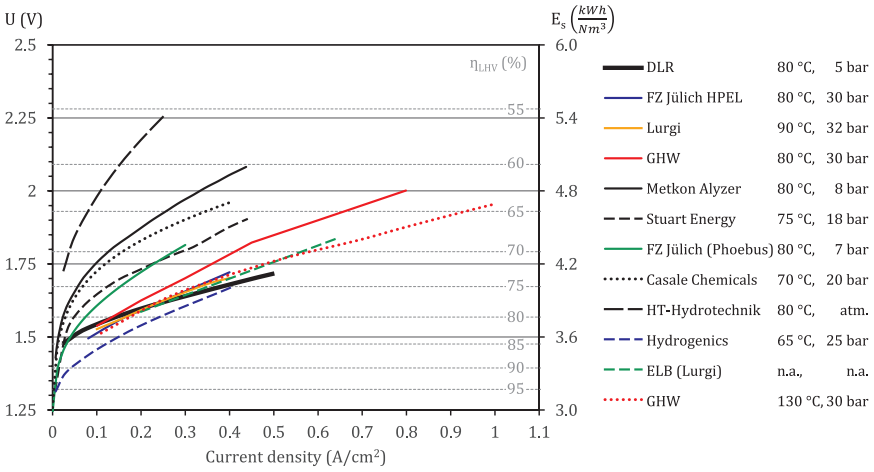

Fig. 6. Overview of characteristic I-U-curves of alkaline electrolysis from literature [16,19,23,36,70,101,102,115].

range as AEL but at a higher current density. At a current density of 0.1 A/cm^2 (5% based on a nominal current density of 2 A/cm^2) the efficiency of the presented PEMEL cells increases to 76–84%, based on LHV (U = 1.5–1.65 V, E_s = 3.6–3.9 kW h/Nm^3).

Overall system performance of a pilot plant is presented in detail by Hydrogenics for the DonQuichote project [97]. The mean specific consumption (DC) of the stack is stated to be 4.47 kWh/Nm^3 (η_{LHV} = 67%) for a transient operated 30 Nm^3/h PEM electrolyser. The specific energy consumption of the system (including utilities and rectification with a poor mean efficiency of 88%) is given to be 5.25 kWh/Nm^3 (η_{LHV} = 57%) and 5.55 kW h/Nm^3 (η_{LHV} = 54%) including compression to 450 bar. The power consumption of the utilities in stand-by is approx. 1 kW, which corresponds to less than one percent of the nominal electrolyser power. Despite the increase in efficiency of the electrolyser in part-load, the overall system efficiency decreases due to the decreasing performance of the oversized compressor. Results of the 6 MW$_{peak}$ PEM electrolysis system from Siemens for the Energiepark Mainz project are shown in Fig. 8. The system efficiency is calculated on the basis of purchased electricity and the higher heating value of measured hydrogen production [108]. It therefore includes rectification and all utilities like cooling, purification and compression to 80 or 225 bar, respectively. As can be seen, the overall efficiency increases from approx. 58% based on HHV (E_s = 6.1 kW h/Nm^3, η_{LHV} = 49%) at peak total power of 6.2 MW (165% of rated power) to 65% (E_s = 5.4 kW h/Nm^3, η_{LHV} = 55%) at rated total power of 3.75 MW. The maximum overall efficiency is reached at 1 MW (27% of rated power) with up to 76% based on HHV (E_s = 4.7 kW h/Nm^3, η_{LHV} = 64%) before it declines very strongly.

An increase in efficiency is possible utilising the low-temperature

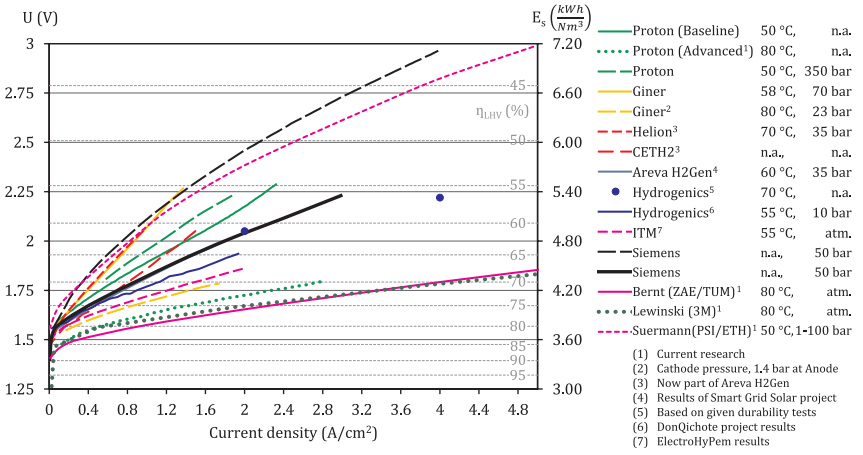

Fig. 7. Overview of characteristic I-U-curves of PEM electrolysis from literature [21,40,90,97,105,107,116–124].

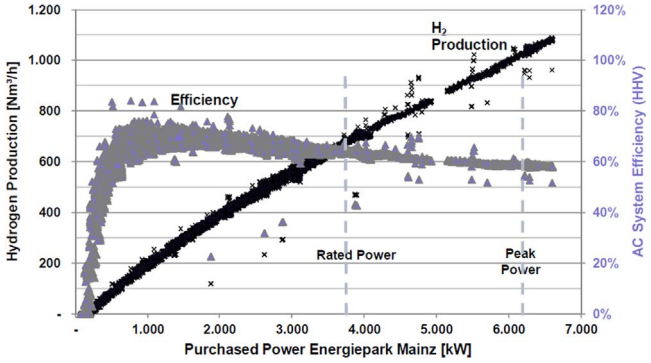

Fig. 8. Efficiency evaluation including all consumers (compression, cooling, purification, control) of the Siemens PEM electrolysis system at Energiepark Mainz [108].

waste heat of the electrolyser and integrating the by-product oxygen. Heat integration has been demonstrated for example within the Stromlückenfüller project (PEM electrolysis by H-TEC) [109] and the RWE's Ibbenbüren power-to-gas plant (PEM electrolysis by ITM) [88] stating an overall energy utilisation (including heat) of 95% and 86% (based on HHV), respectively. In the BioCat project, featuring 2 × 500 kW AEL of Hydrogencis, the capability and economic viability of the integration of by-product oxygen and waste heat in a biogas plant should be shown [110].

As previously discussed, operating temperature has a strong influence on stack efficiency. An increase in temperature corresponds to a reduction in cell voltage or specific energy consumption of 0.01–0.1 V/

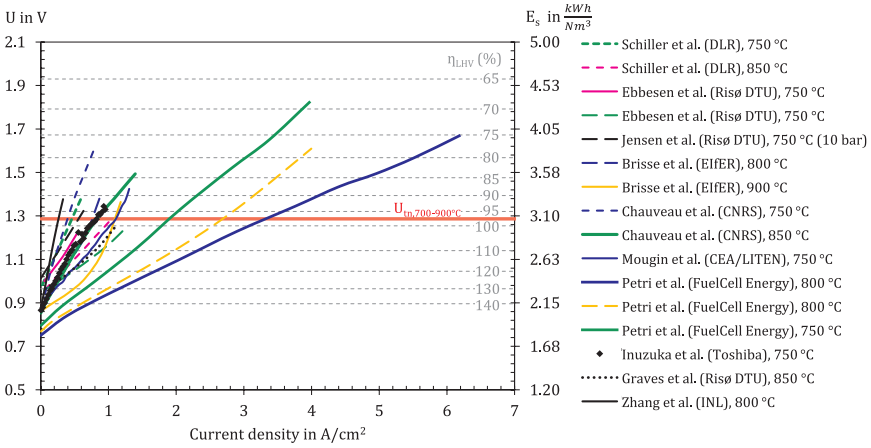

Fig. 9. Overview of characteristic I-U-curves of solid oxide electrolysis from literature [24,59,111,112,125–130].

10 °C or 0.02–0.24 kW h/Nm^3/10 °C for AEL and PEMEL respectively (based on I-U curves determined at different temperatures from literature [16,21,23,25,97,100–102]). However, the temperature-related increase in efficiency is reduced at higher temperatures. Pressure has only a little influence on stack efficiency, which will be discussed in the next section.

Comparison of characteristic I-U-curves of SOEL is more difficult than for AEL and PEMEL. On the one hand, SOEL I-U-curves are dependent on further parameters such as steam conversion rate (rising at higher current density at given feed flow rate or decreasing at higher feed flow rate at given current density), feed composition (humidity, inert gases) and sweep gas on the oxygen side [42,45,111,112]. On the other hand, significant differences between single-cell and stack tests are observed in some cases due to the research state of SOEL [24,45,113]. Because of this, the I-U-curves of SOEL presented in Fig. 9 are only aimed to provide an orientation of the performance. As can be seen, most of the solid oxide cells are operated at up to 1 A/cm^2, mainly due to degradation issues. Exceptions are the results measured by FuelCell Energy up to a current density of above 6 A/cm^2, although long-term tests presented by FuelCell Energy are also carried out below 1 A/cm^2 [59]. However, this shows the potential of SOEL to be operated at thermoneutral cell voltage at much higher current densities once degradation is reduced [52]. Several SOEL cells have been operated below thermoneutral cell voltage due to current density limitation by degradation issues. However, a thermoneutral cell voltage of approx. 1.28 V at 700–900 °C represents the nominal operation point of SOEL. This corresponds to a specific energy consumption of approx. 3.1 kWh/Nm^3 or an efficiency of 98% based on the LHV. Additionally, the external supply of steam, which can be generated by heat integration, has to be taken into account. The overall efficiency including water evaporation of an ideal SOEL system (without losses) is limited to 84.6% based on LHV (100% based on HHV). Mathiesen et al. [114] estimated the efficiency of an SOEL system to be approx. 76.8% based on the LHV including losses (rectifier losses, surface heat losses and auxiliary heating). The specific energy consumption of the overall system of Sunfire, including gas purification and rectification, is stated to be 3.7 kWh/Nm^3, which corresponds to an efficiency of 81% based on LHV [96].

A summary of the stack performance of AEL, PEMEL and SOEL based on the I-U-curves presented before is shown in Fig. 10 (stack-efficiency is calculated based on given cell voltages, assuming an ideal Faraday efficiency of 100%). It shows the high efficiency of SOEL cells, as well as the comparable efficiency of AEL and PEMEL, with PEMEL reaching significantly higher current densities. The potential to reduce capital costs by increasing current density (higher production per cell area) and cutting operational costs by increasing efficiency is discussed in Section 5.6.

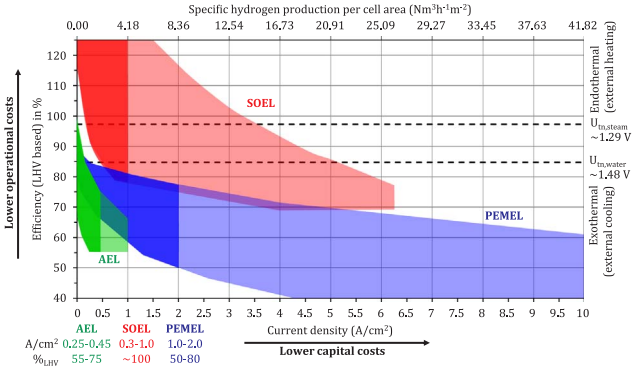

Fig. 10. Summary of efficiency and operational range of AEL [16,19,23,36,70,101,102,115], PEMEL [21,40,90,97,105,107,116–124] and SOEL [24,59,111,112,125–130] cells or stacks.

5.2. Pressurised operation

Hydrogen is usually stored or utilised (e.g. methanol synthesis) at high pressure. If the pressurised operation of electrolysis has the potential to increase the efficiency and to reduce the investment and maintenance costs is discussed controversially in literature [36,131,132].

On the one hand liquid compression of water is more efficient than compression of the gaseous products [131] and pressure has only a minor impact on electrolyser performance [21,111,117,119,124,133,134]. Higher pressure operation slightly increases the reversible cell voltage (decreases the internal heat integration) but results in smaller gas bubbles at the electrode surface thus reducing the related overvoltages [18,100]. Ayers et al. report that increasing the pressure from 14 bar to 165 bar results in an increase in cell voltage of less than 50 mV (approx. 0.1 kWh/Nm^3) [132]. Based on these experiments, they calculated that electrochemical compression via PEMEL up to 70 bar followed by mechanical compression is energetically optimal for a delivery pressure of 350 bar. The elimination of the compressor increases reliability and reduces investment costs and maintenance especially for small-scale systems [132,135]. However, increased pressure leads to higher degradation [36,136], higher cross permeation corresponding to an efficiency penalty and a safety issue (risk of a flammable gas mixture) thus increasing the minimum load range [17,18,137,138] and higher gas leakage [36]. Grigoriev et al. proposes modified membranes (low-permeability protective layer, thicker membranes) platinized backside surface of the current collector or external catalytic gas recombiner to avoid a critical contamination in PEMEL [18]. Moreover, high pressure electrolyser require additional safety devices and result in higher investment costs and complexity of the electrolyser [7,36].

As a result, the standard pressure of commercial AEL and PEMEL is below 30–50 bar in most cases (see Table 2). However, also very high pressure operation at 5000–6500 psig (345–448 bar) for direct filling of hydrogen cars is investigated and was demonstrated for alkaline electrolysis by the company Avalance LCC [64,135,139] as well as for PEM electrolysis by the companies Giner Inc. [40] and Proton Onsite [39]. It represents a huge challenge for AEL to reach a reliable gas purity at high pressure operation due to cross-permeation [64,135,137]. In contrast, Proton and Giner were able to demonstrate reliable PEMEL operation even at a high differential pressure as a result of the low permeation across the membrane [39,40]. The hydrogen side was operated at 170 or 345 bar respectively while the oxygen side was operated at atmospheric pressure. Recently also pressurised operation of SOEL was investigated by several research groups [111,133,140,141] at pressure up to 15 bar and Sunfire offers a commercial module operated at 15 bar [96].

5.3. Available and realised capacity ranges

Electrolysis is used primarily for small-scale on-site hydrogen production in industrial applications e.g. for hydrogen cooled generators, semiconductor or food processing. On the other hand, fertiliser plants based on large-scale (100–200 MW) alkaline electrolysis have been constructed in the 20th century in remote areas with excess electricity supply from large hydro plants in combination with a weak grid. Main examples are Assuan (Egypt) in 1960 (40,000 Nm^3/h, 288 electrolysers, > 200 MW_{el}), Nangal (India) in 1961 (30,000 Nm^3/h), Glomfjord (Norway) in 1949 (27,100 Nm^3/h), Rjukan (Norway) in 1929 (27,900 Nm^3/h) and Kwekwe (Zimbabwe) in 1974 (pressurised AEL, 21,000 Nm^3/h, 28 electrolysers) [7,26,34,71].

Energy storage and carbon utilisation represent an emerging market for electrolysis requiring very large capacities (multi MW systems). Large electrolysis plants in the multi MW range are built up by electrical parallel arrangement of electrolysis stacks typically accommodated indoor. On the other hand several manufacturers of electrolyser offer “plug and play” units in 20 ft or 40 ft container including water purification, power supply, hydrogen purification and system control up to a hydrogen production rate of 100–400 Nm^3/h (0.5–2 MW) [38,73,83,86,88,89,94].

While alkaline electrolysis stacks have been available on a MW-scale for a long time, a scale-up of PEM electrolysis has been realised in the last few years, driven by PtG and PtL. The market survey indicates that currently AEL stacks are available up to 6 MW (1400 Nm^3/h), PEM stacks up to 2 MW (400 Nm^3/h) and SOEL stacks in a low kilowatt range. Moreover, Siemens recently announced a new product line with a single stack capacity of 6 MW to be installed in the H2Future project [142]. MW-scale stacks are provided by 12 manufacturers of AEL and 3 manufacturer of PEMEL (Giner, Hydrogenics, and Siemens). Additionally, Proton Onsite and ITM offer standardised PEM electrolysis systems on the MW-scale, consisting of several stacks.

Cell area, nominal current density and number of cells determine the production rate of a single stack. Currently, the active cell area of PEMEL (< 0.13 m^2 [86,89–91,120]) and SOEL (< 0.06 m^2 [41,44,58,59,125,128,143,144]) is of one and two orders of magnitude smaller than AEL (up to 3–3.6 m^2 [33,34,70]). The higher nominal current densities of PEMEL and SOEL compared to AEL partly offset the lower cell area.

An analysis of flexible electrolysis in PtG and PtL pilot plants presented in Fig. 11 shows that recently, several plants larger than 1 MW were realised with PEMEL catching up to AEL. Examples of large-scale PEMEL projects are the Energiepark Mainz commissioned in 2015 (DE, 6 MW, Siemens), WindGas Haßfurt in 2016 (DE, 1.25 MW, Siemens) and WindGas Hamburg in 2015 (DE, 1 MW, Hydrogenics). Large-scale AEL pilot plants were realised in the Audi e-gas power-to-gas plant in Werlte in 2013 (DE, 6.3 MW, McPhy), the commercial George Olah Renewable Methanol Plant in Svartsengi in 2012, which was expanded

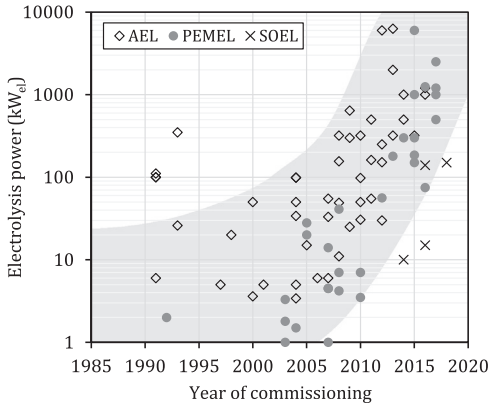

Fig. 11. Installed electrolysis power of flexible PtG and PtL pilot plants (own illustration based on [2,88,108,145–148]).

in 2015 (IS, 6 MW, n.a.) and the EON demonstration plant in Falkenhagen in 2013 (DE, 2 MW, Hydrogenics). The largest SOEL pilot plant to date is a 140 kW system of Sunfire delivered to its partner Boeing and commissioned at a US navy microgrid test facility in 2016.

5.4. Flexibility

Transient operation of the electrolysis section to react to electricity price variations is the basis of both PtG and PtL energy storage. Flexibility is defined by a feasible load range (minimum load and overload possibility), the load gradients, start-up time (warm, cold) and stand-by losses. However, an agreement on terminology (stand-by, idle, cold start, black start, warm start) is required, according to electrolyser companies [4,149]. In the following, a warm start is defined as start-up from heated stand-by or idle mode, which means that the system is held at operating temperature and pressure if necessary. A cold start is defined as start-up from ambient temperature after a long shut-down.

5.4.1. Load range

In practice, large-scale electrolysis systems consist of several electrolysers in parallel. Therefore, it is possible to vary the power consumption of the overall system over a wide range by switching off individual electrolysers.

The minimum load of AEL is limited to 10–40% (mainly 20–25% based on Table 2) of nominal hydrogen production due to the lateral diffusion of hydrogen across the membrane to the oxygen side, resulting in a flammable mixture at low production rates [19,20]. In practice, safety shut-downs take place at a hydrogen contamination of 1–2% in the oxygen stream [6,37,99,100], corresponding to approx. 25–50% of the lower explosive limit, which is in the range of 4–6% H_2 in O_2, depending on temperature and pressure [137]. Reported contamination by dissolved gases in the mixed circulating electrolyte streams is not relevant due to the shut-down of electrolyte circulation for heat removal in part-load [7,37]. For PEM electrolysis, most suppliers state no technical limit of minimum load due to the low gas permeability of the membrane. However, at high pressure (or due to thinner membranes for improved performance) PEMEL also faces critical gas contamination at low current densities [17]. Several vendors of PEMEL have advertised the possibility of overload operation. However, this is dependent on the definition of nominal load (nominal current density) and requires power supply and thermal management to be dimensioned for maximum load [150]. The impact of overload on long-term performance has yet to be investigated (increased degradation at high overpotentials has to be considered).

In case of SOEL, reversible operation is possible, allowing for an operating range of −100 to 100% [96]. However, if the cell is operated below thermoneutral voltage, external heat must be supplied to prevent the stack from cooling. Air sweep and electric heaters have been

considered for the temperature control of the electrolysis cells [47,151].

5.4.2. Transient operation and grid balancing capability

In general, electrolysis systems can be operated very dynamically, limited mainly by the heat management, the maximum voltage of the rectifier and the time coefficients of external components [7,37]. Running PEMEL and AEL systems at nominal temperature can vary their full load range from less than one second to a few seconds [6,19,33,74,87,99,100,104,118,121]. This permits both PEMEL and AEL for grid balancing service. PEMEL and AEL performed similarly in frequency-regulation experiments at NREL [152]. Results show that both the PEM and alkaline electrolysers are capable of adding or removing stack power to provide a sub-second response that reduces the duration of the frequency disturbances in a microgrid. Hydrogenics, offering AEL and PEMEL technology, states that both technologies can react very rapidly (power response signal < 1 s) to stabilise power grids when the system is running and at operating temperature [83]. Frequency regulation was demonstrated by Hydrogenics with an alkaline electrolyser in the Ontario Grid [121]. Within the Thüga project, the 300 kW PEM electrolyser provided by ITM could be prequalified for primary grid balancing in Germany in 2016 [153].

5.4.3. Cold and warm start-up

For flexible operation, PEMEL and AEL are held on temperature in stand-by mode due to the lower electrochemical performance in cold operation and the required time for heat-up. Moreover, Reissner et al. report that some large-scale alkaline models have to be held above a minimum temperature to ensure the leak-tightness of the electrolyser block [154]. Warm start-up time from heated and pressurised stand-by mode to full load is possible within 1–5 min for AEL [6,33,37,70,100,155,156] and within seconds for PEMEL [6,38,87,90,105,155]. On a MW-scale, less than 10 s from idle or stand-by mode to full load are reported by Siemens and Proton Onsite [87,105].

The 6 MW alkaline electrolysis unit (3 × 2 MW) of the Audi e-gas plant Werlte, which is held on temperature in stand-by through heat integration with a biogas plant, can be started from 0 MW to 6 MW within 4 min [157]. However, the risk of product gas contamination by dissolved gases carried by the mixed lye streams being circulated for heat integration has to be considered. Jensen et al. report that pressurised Lurgi electrolysers can be shut down for up to 4–6 h without losing pressure or temperature and without reducing the operating life [6].

The heat-up time of the electrolyser determines the time for cold start-up. A free variation of power of an alkaline electrolyser is typically possible above a temperature of 50 °C [37,100]. The heating of the electrolyser by internal losses is limited by the maximum current or the maximum voltage of the rectifier, as well as by corrosion at high voltages or current densities respectively [37,100]. The maximum voltage becomes limiting at low operating or start-up temperature as this results in high overpotentials during start-up. Therefore, a cold start results in high cell voltages at low current densities limiting the maximum power (P=U I) of the electrolyser at the beginning [37,100]. Heat-up experiments on a small alkaline electrolyser (Hydrogencis HySTAT-1 Nm^3/h, approx. 5 kW) have been conducted by Dieguez et al., indicating heat-up times of more than 2 h from 20 °C to 70 °C at a maximum current density of 0.4 A/cm^2 [101]. In contrast, experiments by Zuberbühler et al. with a HySTAT-60 electrolyser show heat-up times from 15 °C to 50 °C of 1.25 h at the minimum current density of 0.175 A/cm^2 and only 24 min at the maximum current density of 0.43 A/cm^2 (37 min from 15 to 70 °C). At maximum current density, a heat-up ramp of 1.5 K/min of the small-scale 15 Nm^3/h stack was achieved. For large-scale industrial AEL plants designed for continuous operation, necessary heat-up times of 2 h have been reported [6,156]. According to Mr. Hug from Wasserelektrolyse Hydrotechnik, a reduction in heat-up time to 1 h could be demonstrated by auxiliary heating [37]. For some commercial alkaline models, the power increase is limited at low temperature to ensure the stack and system leak-tightness and to minimise mechanical stress to the system due to rises in operating temperature [154].

PEMEL have shorter heat-up times compared to AEL following from the more compact design and lower thermal capacity and in some cases lower operating temperature [25,97]. In the Don Quichote project. thermal ramps of 0.3–1 °C/min, depending on the current applied, are presented for a 30 Nm^3/h PEM electrolyser [97]. Stated cold start-up times to full load for PEMEL systems are in the range of 5–10 min [38,87,90,155].

A SOEL module has to be held at the high operating temperature of 700–900 °C in idle mode [96]. Otherwise a long start-up time is necessary to heat the system up and to avoid the risk of thermal stress [7]. Sunfire claims that flexible operation from 1% to 100% in 15 min is possible when the system is at operating temperature [61]. Load cycling experiments of reversible solid oxide cells (−100 to 100%) were presented by Sunfire [44], Haldor Topsoe [60] and Fuel Cell Energy [59] showing only slight degradation (0.06%/cycle). Petipas et al. [158] showed that SOEC can be operated under on-off conditions without increased degradation rates. Mougin et al. [128] carried out on-off tests and thermal cycling (20–800 °C, 1 °C/min) on a three-cell stack, showing only minor degradation. However, it has to be taken into account that the presented experiments of dynamic operation of SOEL are based on laboratory test benches in order to investigate the impact on cell degradation. Transient operation of a SOEL system is more difficult due to the complex thermal management of the overall system including heat recuperation.

5.4.4. Stand-by losses

Losses by dynamic operation of electrolysis units result from:

- Purging the gas compartments after a longer shut-down for safety reasons (especially relevant for pressurised alkaline electrolysers due to cross permeation) [36,99,154]
- Applying a protective current in stand-by to avoid degradation
- Optional heating in stand-by mode to guarantee a fast reaction time.

For SOEL especially, it is very energy consuming to hold the system on temperature but Petipas et al. [158] showed that SOEL does not require a protection current.

Depending on the electrode activation, a protective current is necessary in stand-by mode for AEL [9,19,159,160]. In the Res2H2 project it is reported that a protective current consuming 0.35 kW for a 25 kW electrolyser is recommended by the manufacturer Casale [104]. However, no degradation has been indicated after two years of intermittent operation without applying the recommend protective current due to the use of corrosion-resistant activated electrodes. Personal communications with Mr. Barisic from ELB and Mr. Hug from Wasserelektrolyse Hydrotechnik revealed that both manufacturers use electrodes that do not require a protective current [37,156].

Zuberbühler et al. state that the Hydrogenics HySTAT alkaline electrolyser holds the pressure in stand-by mode for several days (and even weeks) permitting a start-up without any prior inert gas purging of the gas ducts [100].

According to Siemens, no inert gas flushing, no protective current and no preheating is required for their PEMEL technology [108], while Areva H2Gen reported a pressure loss of only 2.5 bar over more than 12 h of a pressurised PEM at 35 bar held in heated stand-by [90].

5.5. Lifetime

Lifetime is an important parameter for the economic analysis of electrolysis systems and voltage degradation results in reduced performance during operating life. In the following, an overview of technology related values of lifetime is given and the dependency on operating conditions (pressure, temperature, current density, intermittent

operation) is discussed.

Regarding the lifetime of an electrolyser, it has to be distinguished between the stack and the plant. Balance of plant has a typical lifetime of about 20 years [89,98,129,161] for SOEL and PEMEL with up to 30–50 years stated for stationary operated AEL [30,31,37,70]. The increase in overpotentials or the decrease in efficiency with time due to degradation of the cells determines the lifetime of the stack based on a defined, acceptable efficiency drop (e.g. less than 10% efficiency loss after 60,000 h [106]). A replacement or partial overhaul of the cell stack is typically required after 8–15 years for AEL [32,37,70,72]. Felgenhauer and Hamacher [162] report a stack lifetime of 55,000–96,000 h at an efficiency degradation of 0.25–1.5%/a, based on 11 quotes for commercial AEL systems in 2014. ELB reports an annual voltage degradation of 10–15 mV (approx. 1–2 μV/h corresponding to 0.5–1%/a efficiency degradation) [70]. Manufacturers of PEMEL report lifetimes in the range of 60,000–100,000 h [40,105,106,108,162]. The voltage degradation rate is below 4–8 μV/h [105,107,120,163], which is in line with Felgenhauer and Hamacher [162], who have stated an annual efficiency degradation of PEMEL of 0.5–2.5%/a. In summary, AEL and PEMEL achieve comparable stack lifetimes although PEMEL does tend to have slightly higher degradation rates.

The voltage degradation effectively results in a reduced average efficiency over the lifetime of an electrolyser [4]. Assuming a cell voltage of 1.9 V (η_{LHV} = 66.0%), a linear voltage degradation of 2–4 μV/h over a lifetime of 80,000 h results in a cell voltage of 2.06–2.22 V (η_{LHV} = 56.5–60.9%) at end-of-life (approx. 5–10% points below start of life). This corresponds to an average efficiency of 61.2–63.5%, which is approx. 3–5% below the efficiency at the start of life.

In contrast to AEL and PEMEL, only limited long-term experience mainly based on SRU (single repeat units), single cells or short stacks (< 10 cells) is available for SOEL. Most of the durability tests reported in literature are below 5000 h. The longest experiment reported so far in literature of more than 16,000 h was conducted at the European Institute for Energy Research (EIFER) in the context of the SUNFIRE project [52,61]. The average degradation rate in this single cell test was below 0.6%/1000 h (< 7.3 μV/h) at current densities up to 0.9 A/cm^2 (T = 847 °C, steam conversion 51%). This is within the range of the lowest available values for SOEL and close to the degradation rates of PEMEL. At the start of life, the cell is operated below thermoneutral voltage at 1.185 V (determined by the applied current density of 0.9 A/cm^2). Based on the stated degradation rate, the thermoneutral voltage is calculated to be reached after 17,000 h of operation. Assuming an identical degradation in a stack environment, this corresponds to about two years of operation without any increase in overall electrical consumption. The increasing consumption of the stack is compensated for by a reduced electrical heating demand to maintain the temperature of the stack. Topsoe Fuel Cell, H2Logic and Riso DTU report a state-of-the art stack lifetime of 8000 h for SOEC in the planSOEC project report [164].

Based on a good overview of durability results from literature by Mougin [113], current degradation rates of SOEC are mainly in the range of 0.4–6%/1000 h at temperatures of 650–850 °C and current densities of 0.26–1 A/cm^2. FuelCell Energy reported cell degradations for cells with an active area of 81 cm^2 and 550 cm^2 of 0.7% and 3%/1000 h (9 and 33 μV/h) at a current density of 0.5 and 0.36 A/cm^2 [59]. Ebbesen et al. [13] define operation below 1 A/cm^2 as mild conditions. This represents the limit so far of current density to maintain moderate degradation rates [7,128].

Operating conditions have a significant impact on degradation. Degradation is increased at higher current densities and increased temperature [113,136]. In the case of SOEL, degradation also tends to increase at higher steam concentration and higher steam conversion [13,113]. With regard to PtG or PtL applications, the impact of transient operation on lifetime is relevant. Several manufacturers report that load cycling has no significant effect on the lifetime of PEMEL [108,120,165]. This has also been reported for SOEL based on initial cell experiments [128,158]. Recent investigations by Rakousky et al. have revealed that the degradation of PEMEL can even be reduced by intermittent operation [166]. Variation of the current density is found to have a positive effect on durability, as it lets reversible parts of degradation recover. However, short cycling intervals of 10 min show higher degradation than long intervals of 6 h. For the reversible operation of SOEL, a cycle degradation rate of 0.06%/cycle (−0.38/+0.31 A/cm^2) has been observed by experiments by Sunfire [61] and approx. 0.02%/cycle (0.03 mV/cycle at +/− 0.3 A/cm^2) by FuelCell Energy [59].

The effects of transient operation on stack and system lifetime are not yet well quantified [4] and systematic studies to quantify the impact of operating parameters on durability and to understand the degradation mechanisms are still necessary [113].

5.6. Investment and maintenance costs

The electrolysis section represents a major proportion of the investment costs of a PtG or PtL plant. The overview of investment costs presented in the following is based on market surveys by Jensen et al. (2008) [6], Smolinka et al. (2011) [7], Dahl et al. (2013) [8], E4tech (2014) [4] and Felgenhauer and Hamacher (2015) [162].

E4tech reports that the combined capital costs include electrolyser stack, gas water separator, gas drying (H_2 purity above 99.4%), water management, lye system (AEL), system control and power supply but exclude installation, grid connection, external compression, external purification and hydrogen storage [4]. Smolinka et al. (2011) [7] also give uninstalled costs while the data from Jensen et al. [6] and Dahl et al. [8] is not specified. The values given by Felgenhauer and Hamacher [162] are based on 16 quotes by electrolyser manufacturers in 2014 and include all the necessary auxiliary components, such as feed water treatment, cooling system, hydrogen purification for a hydrogen purity above 99.999%, shipping, foundation/shelter and the “turnkey” installation. Smolinka et al. assume that the additional costs for installation and transportation would be approx. 10% of the investment costs [7]. The investment costs of AEL and PEMEL are shown in Fig. 12.

Installed system costs of large-scale AELs above 500 kW are currently mainly in the range of 800–1500 €/kW$_{el}$. Uninstalled costs are slightly lower, mainly in the range of 700–1300 €/kW$_{el}$. PEMEL system costs are almost twice as high with given uninstalled costs ranging from 1300 to 2200 €/kW$_{el}$. The installed costs calculated based on Felgenhauer and Hamacher [162] are in the same range as the uninstalled costs stated by others at 1400–2100 €/kW$_{el}$.

The economy-of-scale effect is limited for electrolysis systems. The hydrogen production rate is linearly dependent on the electrolysis cell area and mainly the specific costs of the auxiliaries reduce at increased scale. Market surveys by Smolinka et al. [7] and Jenssen et al. [6] indicate that a significant effect of scale for AEL systems is only visible at capacities below 0.5 MW (100 Nm^3/h) and further cost reductions above this scale are low. However, Proton Onsite reports that a scale-up of their PEMEL system from 0.5 to 2 MW almost halves the specific costs per kW although the cost trajectory flattens above 0.5 MW [167].

In the future, a cost reduction is expected from the higher volume production of electrolysers, the supply chain development, improvements in manufacturing (increased automation) and technology innovations [4]. Reduction in capital costs by increased current densities and reduction in operating costs through higher efficiency at higher operating temperatures are often mentioned. However, the impact on lifetime and degradation also has to be taken into account. The formation of gas bubbles limits the current density of AEL, as it reduces the effective active electrode area. Development of catalysts with increased current exchange rates and the application of advanced cell designs such as zero gas configurations are required to overcome this problem [4]. PEMEL has the potential of cost reduction by increased cell areas reducing the waste material, a decrease in the noble metal content of the electrodes and alternative membrane materials and flow field plates [4,11,106,167].

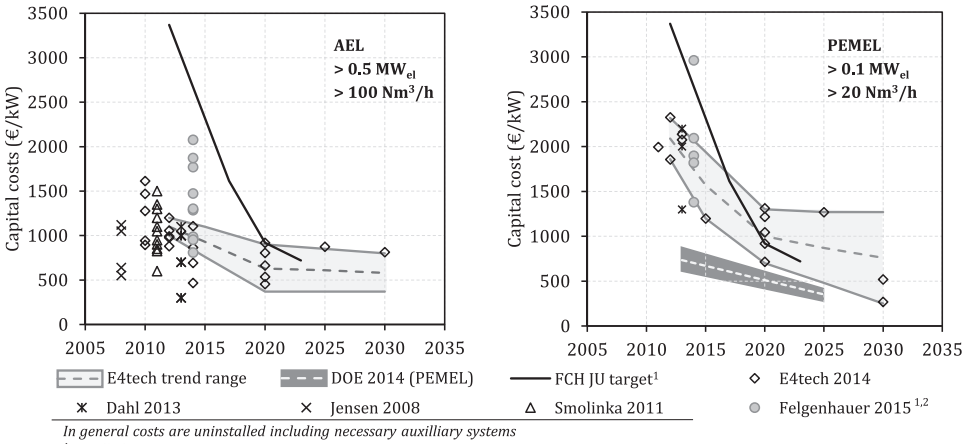

In general costs are uninstalled including necessary auxilliary systems
[1]Installed costs
[2]reported costs in €/kWh$_{H2}$ are converted to €/kW$_{el}$ based on the assumption of a specific energy consumption of 5 kWh$_{el}$/Nm^3

Fig. 12. Current capital costs, expected future trend and targets for AEL and PEMEL systems (based on [4,6–8,15,162,169]).

In the E4tech study [4], cost reduction trend lines are derived based on stakeholder consultations. In the mid-term a cost reduction in AEL to about 630 €/kW by 2020 and 580 €/kW by 2030 is expected (central case). The uninstalled system costs of PEMEL are predicted to fall to 1000 €/kW by 2020 and 760 €/kW by 2030.

Due to the pre-commercial status of SOEL, there is a high level of uncertainty about investment costs. E4Tech [4] states expected commercial costs of 2000 €/kW$_{el}$ between 2012 and 2020, 1000 €/kW$_{el}$ between 2020 and 2030 and 300 €/kW$_{el}$ in the longer term. A recent DOE report [168] even assumes uninstalled capital costs of approx. 640 €/kW$_{el}$ in 2014 and below 340 €/kW$_{el}$ by 2025 for a large-scale central plant (50,000 kg/day).

The operational cost per year including planned and unplanned maintenance, as well as overhauls (excluding electricity) are often provided, based as a percentage of initial capital expenditure (capex). The E4tech study reports opex (operational expenditure) values of 2–5% of capex per year with no distinction between different technologies [4]. Based on own calculations using the opex data given by Felgenhauer and Hamacher. [162] eight of the AEL quotes provide opex values of 2–3% of capex per year while three quotes state opex values in the range of 5–6% of capex per year. The five quotes for PEMEL system have opex values of 3–5% of capex per year. This corresponds to higher operational and maintenance costs of PEMEL compared to AEL due to the higher capex of PEMEL. Moreover, the specific opex values per installed capacity show a similar trend as the capex, tending to decrease with the size of the electrolysis system [162].

6. Conclusions

The main parameters of the water electrolysis technologies investigated (AEL, PEMEL and SOEL) are summarised in Table 3. Alkaline electrolysis (AEL) represents the most mature technology, having been commercial available for over a century. It has the lowest specific investment and maintenance costs. Twenty manufacturers of AEL could be identified that offer single-stack capacities up to 6 MW. Historically, AEL was designed for stationary applications and has to be adapted to the new flexibility requirements. In contrast, the development of PEMEL has been driven very strongly by flexible energy storage application in recent years. PEMEL has entered the MW class and several pilot plants in the MW range up to 6 MW have recently been realised. Twelve manufacturers of PEMEL could be identified, with three offering stacks on the MW scale (with two other manufacturers with systems on the MW-scale). PEMEL offers several advantages compared to AEL with regard to compact design (high current-densities), pressurised operation and flexibility. PEMEL features shorter start-up times, especially from cold, and the production rate can be varied over the full load range. In contrast, the load range of AEL is limited to approx. 20–25% due to the risk of a flammable mixture arising due to cross contamination of the product gas streams. However, grid stabilising could be demonstrated by PEMEL and AEL systems as both offer very fast load dynamics (response < 1 s) when they are at operating temperature.

In the future, the mode of operation needs to be further optimised for dynamic operation and the impact of flexible operation on lifetime has to be investigated in more detail. The integration of electrolysis systems in other processes, such as biogas plants, fuel synthesis or industrial processes (e.g. steel manufacturing) has been demonstrated in initial projects. Further projects are required to indicate interesting buisness cases and to investigate the potential for generating synergy effects by integrating waste heat or oxygen as a by-product. Investment costs are likely to fall in the future due to the higher volume production of electrolysers, supply chain development, improvements in manufacturing (increased automation) and technology innovations (e.g. increased current density, reduction in expensive materials for PEMEL) supporting the competitiveness of electrolysis against other storage options.

Table 3
Summary of parameters of state-of-the-art of water electrolysis technologies.

	AEL	PEMEL	SOEL
Operation parameters			
Cell temperature (°C)	60–90	50–80	700–900
Typical pressure (bar)	10–30	20–50	1–15
Current density (A/cm^2)	0.25–0.45	1.0–2.0	0.3–1.0
Flexibility			
Load flexibility (% of nominal load)	20–100	0–100	−100/+100
Cold start-up time	1–2 h	5–10 min	hours
Warm start-up time	1–5 min	< 10 s	15 min
Efficiency			
Nominal stack efficiency (LHV)	63–71%	60–68%	100%[a]
…specific energy consumption (kWh/Nm^3)	4.2–4.8	4.4–5.0	3
Nominal system[b] efficiency (LHV)	51–60%	46–60%	76–81%
…specific energy consumption (kWh/Nm^3)	5.0–5.9	5.0–6.5	3.7–3.9
Available capacity			
Max. nominal power per stack (MW)	6	2	< 0.01
H_2 production per stack (Nm^3/h)	1400	400	< 10
Cell area (m^2)	< 3.6	< 0.13	< 0.06
Durability			
Life time (kh)	55–120	60–100	(8–20)[c]
Efficiency degradation (%/a)	0.25–1.5	0.5–2.5	3–50
Economic parameter			
Investment costs (€/kW)	800–1500	1400–2100	(> 2000)[c]
Maintenance costs (% of investment costs per year)	2–3	3–5	n.a.

[a] Operating at thermoneutral voltage.
[b] Including auxiliaries and heat supply (SOEL).
[c] High uncertainty due to pre-commercial status of SOEL.

In contrast to AEL and PEMEL, SOEL is still at pre-commercial stage although the company Sunfire is offering the first pilot plants. SOEL has the potential to increase the efficiency of hydrogen production and offers interesting features as reversible operation and syngas production via co-electrolysis. The development of SOEL systems and the proof of lifetime, pressurised operation and cycling stability have to be continued.

The development of the last few years shows that water electrolysis is on its way to large-scale flexible energy-storage applications.

Acknowledgments

This work is related to the HotVeGas III project, which is supported by the BMWi and industrial partners (Air Liquide and RWE) under contract number 0327773I. The authors would like to thank all the manufacturers of electrolysis systems who we contacted for their valuable input and discussions (especially Mr. Hug of Wasserelektrolyse Hydrotechnik and Mr. Barisic of ELB). Thanks also go to the TUM Graduate School and Stephan Herrmann (TUM) for proofreading as well as Maximilian Möckl (ZAE Bayern) for valuable discussions especially about PEM electrolysis.

References

[1] FCH JU. Commercialisation of energy storage in Europe: Final report; 2015.
[2] Deutsche Energie-Agentur GmbH (dena). Webpage: strategieplattform power to gas. [December 19, 2016]; Available from: ⟨http://www.powertogas.info/⟩.
[3] Klaus T, Vollmer C, Werner K, Lehmann H, Müschen K Energieziel 2050: 100% Strom aus erneuerbaren Quellen; 2010.
[4] Bertuccioli L, Chan A, Hart D, Lehner F, Madden B, Standen E. Development of water electrolysis in the European Union: Final Report; 2014.
[5] Ursúa A, Gandía LM, Sanchis P. Hydrogen production from water electrolysis: current status and future trends. Proc IEEE 2011;99:1–17.
[6] Jensen JO, Bandur V, Bjerrum N, Jensen S, Ebbesen S, Mogensen M et al. Preinvestigation of water electrolysis: PSO-F & U 2006-1-6287, Draft 04-02-2008. [January 31, 2012]; Available from: 130.226.56.153/rispubl/NEI/NEI-DK-5057.pdf.
[7] Smolinka T, Günther M, Garche J. Stand und entwicklungspotenzial der wasserelektrolyse zur herstellung von wasserstoff aus regenerativen energien: kurzfassung des abschlussberichts. NOW-Stud 2011.
[8] Dahl PI, Bünger U, Völler S, Korpas M, Moller-Holst S. Hydrogen for transport from renewable energy in Mid - Norway: Final report; Available from: ⟨http://www.transnova.no/wp-content/uploads/2012/07/H2iMidtNorge_Sluttrapport.pdf⟩.
[9] Stolten D, Krieg D. Alkaline electrolysis – introduction and overview. In: Stolten D, editor. Hydrogen and fuel cells. 1st ed.Weinheim: Wiley-VCH; 2010. p. 243–70.
[10] Zeng K, Zhang D. Recent progress in alkaline water electrolysis for hydrogen production and applications. Progress Energy Combust Sci 2010;36(3):307–26.
[11] Carmo M, Fritz DL, Mergel J, Stolten D. A comprehensive review on PEM water electrolysis. Int J Hydrog Energy 2013;38(12):4901–34.
[12] Hansen JB. Solid oxide electrolysis—a key enabling technology for sustainable energy scenarios. Faraday Discuss 2015;182:9–48.
[13] Ebbesen SD, Jensen SH, Hauch A, Mogensen MB. High temperature electrolysis in alkaline cells, solid proton conducting cells, and solid oxide cells. Chem Rev 2014;114(21):10697–734.
[14] Laguna-Bercero MA. Recent advances in high temperature electrolysis using solid oxide fuel cells: a review. J Power Sources 2012;203:4–16.
[15]. Fuel Cells and Hydrogen Joint Undertaking (FCH JU). Multi - Annual Work Plan 2014 − 2020.
[16] Ulleberg O. Modeling of advanced alkaline electrolyzers: a system simulation approach. Int J Hydrog Energy 2003;28(1):21–33.
[17] Grigoriev SA, Porembskiy VI, Korobtsev SV, Fateev VN, Auprêtre F, Millet P. High-pressure PEM water electrolysis and corresponding safety issues. Int J Hydrog Energy 2011;36(3):2721–8.
[18] Grigoriev SA, Millet P, Korobtsev SV, Porembskiy VI, Pepic M, Etievant C, et al. Hydrogen safety aspects related to high-pressure polymer electrolyte membrane water electrolysis. Int J Hydrog Energy 2009;34(14):5986–91.
[19] Schug C. Operational characteristics of high-pressure, high-efficiency water-hydrogen-electrolysis. Int J Hydrog Energy 1998;23(12):1113–20.
[20] Raballo S, Llera J, Pérez A, Bolcich JC Clean Hydrogen Production in Patagonia Argentina. In: Stolten D, Grube T, (Eds). 18th World Hydrogen Energy Conference 2010 - WHEC 2010: Parallel Sessions Book 3: Hydrogen Production Technologies – Part 2 Proceedings of the WHEC. Schriften des Forschungszentrums Jülich/ Energy & Environment, Vol. 78-3; 2010, p. 10–16.
[21] Bidault C, Besse S, Nietsch T, Chaudron V. Electrolyser development at HELION/ AREVA status & perspectives. Phoenix, Arizona, USA; 2008.
[22] Hug W, Bussmann H, Brinner A. Intermittent operation and operation modeling of an alkaline electrolyzer. Int J Hydrog Energy 1993;18(12):973–7.
[23] Pino FJ, Valverde L, Rosa F. Influence of wind turbine power curve and electrolyzer operating temperature on hydrogen production in wind–hydrogen systems. J Power Sources 2011;196(9):4418–26.
[24] Inuzuka R, Kameda T, Watanabe H, Yamada M. Development of hydrogen production and power storage systems using solid oxide electrolysis cell. Los Angeles, US; 2015.
[25] Smolinka T, Rau S, Hebling C. Polymer electrolyte membrane (PEM) water electrolysis. In: Stolten D, editor. Hydrogen and fuel cells. 1st edWeinheim: Wiley-VCH; 2010. p. 271–89.
[26] Yan XL, Hino R. Nuclear hydrogen production handbook. Boca Raton: CRC Press; 2011.
[27] ErreDue spa. Webpage. [December 13]; 2016. Available from: ⟨http://www.erreduegas.it/en/⟩.
[28] ELB Elektrolysetechnik GmbH. Webpage. [December 13]; 2016. Available from: ⟨http://elektrolyse.de/wordpress/⟩.
[29] Purification Equipment Reseach Institute of CISC (Peric). Webpage. [February 06]; 2017. Available from: ⟨http://www.peric718.com/Products/⟩.
[30] Verde LCC. Webpage. [December 13]; 2016. Available from: ⟨http://www.verdellc.com/⟩.
[31] NEL Hydrogen. If the future could choose: Company brochure. [January 10]; 2012. Available from: ⟨http://www.nel-hydrogen.com/home/docs/If_The_Future_Could_Choose_2.pdf⟩.
[32] Suzhou Jingli Hydrogen Production Equipment Co. L. Webpage. [December 13]; 2016. Available from: ⟨http://www.jingli-hydrogen.com/⟩.
[33] Etogas. Webpage. [December 13]; 2016. Available from: ⟨http://www.etogas.com/⟩.
[34] Wasserelektrolyse Hydrotechnik GmbH. Webpage. [December 13]; 2016. Available from: ⟨http://www.ht-hydrotechnik.de/⟩.
[35] Reissner R, Vaes J, Hosseiny SS. RESelyser: System Concept for a combined RES-Electrolyser plant with optimised efficiency: Part 1 Review of electrolyser system with special emphasis on the HYSOLAR system. [January 04]; 2017. Available from: ⟨http://www.reselyser.eu/⟩.
[36] Roy A, Watson S, Infield D. Comparison of electrical energy efficiency of atmospheric and high-pressure electrolysers. Int J Hydrog Energy 2006;31(14):1964–79.
[37] Hug W. Alkaline electrolysis at wasserelektrolyse hydrotechnik GmbH. Telephone communication; 2013.
[38] Proton OnSite. High capacity hydrogen systems M series PEM electrolysers: MW scale energy storage solutions. [December 12]; 2016. Available from: ⟨protononsite.com/resources/commercial%20brochures/pd-0600-0115_rev_a.pdf⟩.
[39] Ayers KE, Anderson EB, Capuano C, Carter B, Dalton L, Hanlon G, et al. Research advances towards low cost, high efficiency PEM electrolysis. ECS Trans 2010;33:3–15.
[40] Hamdan M. High efficiency large PEM electrolyzers.
[41] Brisse A, Schefold J. High temperature electrolysis at EIFER, main achievements at cell and stack level. Energy Procedia 2012;29:53–63.
[42] Graves C, Ebbesen SD, Mogensen M. Co-electrolysis of CO_2 and H2O in solid oxide cells: performance and durability. Solid State Ion 2011;192(1):398–403.
[43] Saint Jean M, de Baurens P, Bouallou C, Couturier K. Economic assessment of a power-to-substitute-natural-gas process including high-temperature steam electrolysis. Int J Hydrog Energy 2015;40(20):6487–500.
[44] Posdziech O. Development of high-temperature electrolysers for renewable electricity storage. Prague: sunfire GmbH; 2015.
[45] Reytier M, Di Iorio S, Chatroux A, Petitjean M, Cren J, Saint Jean M de, et al. Stack performances in high temperature steam electrolysis and co-electrolysis. Int J Hydrog Energy 2015;40(35):11370–7.
[46] O'Brien JE, McKellar MG, Harvego EA, Stoots CM. High-temperature electrolysis for large-scale hydrogen and syngas production from nuclear energy – summary of system simulation and economic analyses. Int J Hydrog Energy 2010;35(10):4808–19.
[47] Petipas F, Brisse A, Bouallou C. Model-based behaviour of a high temperature electrolyser system operated at various loads. J Power Sources 2013;239:584–95.
[48] Botta G, Solimeo M, Leone P, Aravind PV. Thermodynamic analysis of coupling a SOEC in Co-electrolysis mode with the dimethyl ether synthesis. Fuel Cells 2015;15(5):669–81.
[49] Hansen JB, Christiansen N, Nielsen JU. Production of sustainable fuels by means of solid oxide electrolysis. ECS Trans 2011;35:2941–8.
[50] Giglio E, Lanzini A, Santarelli M, Leone P. Synthetic natural gas via integrated high-temperature electrolysis and methanation: part I—energy performance. J Energy Storage 2015;1:22–37.
[51] Becker WL, Braun RJ, Penev M, Melaina M. Production of Fischer–Tropsch liquid fuels from high temperature solid oxide co-electrolysis units. Energy 2012;47(1):99–115.
[52] Schefold J, Brisse A, Poepke H. Long-term steam electrolysis with electrolyte-supported solid oxide cells. Electrochim Acta 2015;179:161–8.
[53] Buttler A, Koltun R, Wolf R, Spliethoff H. A detailed techno-economic analysis of heat integration in high temperature electrolysis for efficient hydrogen production. Int J Hydrog Energy 2015;40(1):38–50.
[54] Graves C. Recycling CO_2 into sustainable hydrocarbon fuels: electrolysis of CO_2 and H_2O (Ph.D. Thesis); 2010.
[55] O'Brien JE, McKellar MG, Stoots CM, Herring JS. Parametric study of large-scale production of syngas via hightemperature co-electrolysis. INL/CON-07-12819. AIChE annual meeting; 2007.
[56] Stoots C, O'Brien J, Hartvigsen J. Results of recent high temperature coelectrolysis studies at the Idaho National Laboratory. Int J Hydrog Energy 2009;34(9):4208–15.

[57] Alenazey F, Alyousef Y, Almisned O, Almutairi G, Ghouse M, Montinaro D, et al. Production of synthesis gas (H_2 and CO) by high-temperature co-electrolysis of H_2O and CO_2. Int J Hydrog Energy 2015;40(32):10274–80.
[58] Ebbesen SD, Høgh J, Nielsen KA, Nielsen JU, Mogensen M. Durable SOC stacks for production of hydrogen and synthesis gas by high temperature electrolysis. Int J Hydrog Energy 2011;36(13):7363–73.
[59] Petri R, Wood A, He H, Joia T, Brown C, Borglum B. et al. Reversible solid oxide fuel cell (RSOFCEL) development at versa power systems. Los Angeles, US; 2015.
[60] Wonsyld K, Bech L, Nielsen JU, Pedersen CF. Operational robustness studies of solid oxide electrolysis stacks. JEPE 2015;9(2).
[61] Olshausen Cvon. Sunfire – liquid hydrocarbonates from CO_2 and H_2O and renewable energy. Berlin, Germany; 2015.
[62] Olshausen Cvon. Closing the carbon cycle; 2014.
[63] H2Nitidor. Hydrogen-Oxygen high-pressure generator & more … [January 11]; 2017. Available from: 〈www.h2fc-fair.com/hm12/images/exhibitors/h2nitidor001.pdf〉.
[64] Dunn P. high-capacity, high-pressure electrolysis system with renewable power sources. DOE Hydrog Program FY 2010 Annu Progress Report 2010:99–102.
[65] Sioli G Advanced water electrolysers power by renewable energy sources; Available from: 〈http://www.casale.ch/images/casalegroup/events/paper_archive/chemicals/2004/h2_age_pisa_italy_2004_advanced_water_electrolysers_powered_by_renewable_energy_sources.pdf〉.
[66] Thyssen Krupp AG. Water electrolysis: Power to gas. [February 04]; 2017. Available from: 〈https://www.thyssenkrupp.com/en/company/innovation/technologies-for-the-energy-transition/water-electrolysis.html〉.
[67] Jo M. Hydrogen production activitiesin Japan. Herten, Germany; 2015.
[68] Ceramatec Inc., Webpage. [December 16]; 2016. Available from: 〈http://www.ceramatec.com/〉.
[69] ACTA S.P.A. AES500-1000. [December 16]; 2016. Available from: 〈www.actaspa.com/wp-content/uploads/2013/08/AES500-1000.pdf〉.
[70] Barisic M. Alkalische elektrolyseure – industrielle anwendungen und dynamischer Betrieb. München; 2014.
[71] Industrie Haute Technology (IHT). Webpage. [December 13]; 2016. Available from: 〈http://www.iht.ch/〉.
[72] NEL Hydrogen. Webpage. [December 13]; 2016. Available from: 〈http://nelhydrogen.com/〉.
[73] Next Hydrogen. Webpage. [December 13]; 2016. Available from: 〈http://www.nexthydrogen.com/〉.
[74] Teledyne Energy Systems Inc., Webpage. [December 13]; 2016. Available from: 〈http://www.teledynees.com/〉.
[75] McPhy Energy SA. Webpage. [December 13]; 2016. Available from: 〈http://www.mcphy.com/〉.
[76] Tianjin Mainland Hydrogen Equipment Co. Ltd. Company Webpage. [January 01]; 2017. Available from: 〈http://www.cnthe.com/HT_world/chanpin1_en/index1.asp〉.
[77] Ener Blue SA. Webpage. [December 14]; 2016. Available from: 〈http://www.ener-blue.com/〉.
[78] Uralhimmasch. Webpage: [in Russian]. [December 13]; 2016. Available from: 〈http://en.ekb.ru/〉.
[79] Idroenergy. Data Sheet Modell 120. [December 13]; 2016. Available from: 〈http://www.idroenergy.it/pdf/schede_gen_idr/120.pdf〉.
[80] GreenHydrogen. Webpage. [February 08]; 2017. Available from: 〈http://greenhydrogen.dk/〉.
[81] PURE Energy Centre. Webpage. [December 13]; 2016. Available from: 〈http://pureenergycentre.com/〉.
[82] Hydrogenics. HySTAT Hydrogen Generators: Product brochure. [December 13]; 2016. Available from: 〈http://www.hydrogenics.com/docs/default-source/pdf/2-1-1-industrial-brochure_english.pdf?Sfvrsn=2〉.
[83] Hydrogenics. Renewable Hydrogen Solutions. [December 12]; 2016. Available from: 〈www.hydrogenics.com/wp-content/uploads/HYDROGENICS_RenewableHydrogen.pdf〉.
[84] Sagim SA. Webpage. [December 13]; 2016. Available from: 〈http://www.sagim-gip.com/〉.
[85] Linde AG. ECOVAR® – Standard on-site lösungen: company brochure. [September 10]; 2013. Available from: 〈http://www.linde-gas.de/〉.
[86] Giner Inc. Webpage: high pressure hydrogen generators. [December 12]; 2016. Available from: 〈http://www.ginerinc.com/〉.
[87] Siemens AG. SILYZER 200 (PEM electrolysis system). [December 13]; 2016. Available from: 〈www.industry.siemens.com/topics/global/en/pem-electrolyzer/silyzer/Documents/silyzer-200-en_v1.3_InternetVersion.pdf〉.
[88] ITM Power. Final results presentation. [December 12]; 2016. Available from: 〈www.itm-power.com/wp-content/uploads/2016/08/Results-Aug-2016.pdf〉.
[89] AREVA H2Gen. Webpage. [December 13]; 2016. Available from: 〈http://www.arevah2gen.com/〉.
[90] Gemmer-Berkbilek K. Field test experience with Areva's PEM electrolysis systems. Freiburg, Germany; 2016.
[91] H-TEC Systems. Webpage. [December 13]; 2016. Available from: 〈http://www.htec-systems.de/〉.
[92] Treadwell Corporation. Webpage. [December 12]; 2016. Available from: 〈http://www.treadwellcorp.com/〉.
[93] Angstrom Advanced Inc., Webpage. [December 12]; 2016. Available from: 〈http://www.angstrom-advanced.com/〉.
[94] Kobelco Eco-Solution Co. Ltd. Webpage: Product overview electrolyzer. [December 12]; 2016. Available from: 〈http://www.kobelco-eco.co.jp/product/suisohassei/hhog_seihin.html〉.
[95] Sylatech GmbH. Company Webpage. [December 12]; 2016. Available from: 〈http://www.sylatech.de/〉.
[96] Sunfire GmbH. RSOC Electrolyzer Factsheet. [December 16]; 2016. Available from: 〈www.sunfire.de/〉.
[97] Vaes J. Field Experience with Hydrogenics' Prototype Stack and System for MW PEM electrolysis. Freiburg, Germany.
[98] Saur G, Ramsden T, James B, Colella W. Current Central Hydrogen Production from PEM Electrolysis version 3.0. [January 20]; 2017. Available from: 〈http://www.hydrogen.energy.gov/h2a_production.html〉.
[99] Steeb H, AbaOud H. HYSOLAR: German-Saudi Joint Program on Solar Hydrogen. Production and Utilitzation. Phase II 1992–1995; 1996.
[100] Zuberbühler U, Specht M, Stürmer B, Brinner A, Brellochs J, Feigl B. et al. Verbundprojekt Power-to-Gas - Errichtung und Betrieb einer Forschungsanlage zur Speicherung von erneuerbarem Strom als erneuerbares Methan im 250 kWel Maßstab. Schlussbericht zum Teilvorhaben; 2014.
[101] Dieguez P, Ursua A, Sanchis P, Sopena C, Guelbenzu E, Gandia L. Thermal performance of a commercial alkaline water electrolyzer: experimental study and mathematical modeling. Int J Hydrog Energy 2008;33(24):7338–54.
[102] Wasserelektrolyse Hydrotechnik GmbH. Produktdatenblatt Elektroylseur Typ EV 50. [January 06]; 2017. Available from: 〈www.ht-hydrotechnik.de/fileadmin/Datenblaetter/Produktdatenblatt_EV_05-13c.pdf〉.
[103] Gammon R, Roy A, Barton J, Little M. Case Study - Hydrogen and Renewables Integration (HARI): IEA–Hydrogen Implementing Agreement; 2006.
[104] Mentado D, Ramirez P, Suarez S, Piernavieja G RES2H2 − 2007 Final technical report; 2008.
[105] Anderson E. PEM electrolyzer reliability based on 20 years of product experience in commercial markets. Freiburg, Germany; 2016.
[106] Pewinksi P. AREVAH2Gen - PEM Electrolyser cost reduction strategy. Herten, Germany; 2015.
[107] Lewinski KA, van der Vliet D, Luopa SM. NSTF advances for PEM electrolysis - the effect of alloying on activity of NSTF electrolyzer catalysts and performance of NSTF based PEM electrolyzers. ECS Trans 2015;69(17):893–917.
[108] Schönberger D. P2G durch Elektrolyse – eine flexible Speicherlösung. Zürich; 2016.
[109] Joule GP. Stromlückenfüller. [January 17]; 2017. Available from: 〈https://www.gp-joule.de/fileadmin/Content/Downloads/DE/Produktblaetter/Stromlueckenfueller_DE.pdf〉.
[110] Thomas D. Electrolyzer technology of the BioCat project. Copenhagen; 2016.
[111] Jensen SH, Sun X, Ebbesen SD, Knibbe R, Mogensen M. Hydrogen and synthetic fuel production using pressurized solid oxide electrolysis cells. Int J Hydrog Energy 2010;35(18):9544–9.
[112] Ebbesen SD, Graves C, Mogensen M. Production of synthetic fuels by co-electrolysis of steam and carbon dioxide. Int J Green Energy 2009;6(6):646–60.
[113] Mougin J Hydrogen production by high-temperature steam electrolysis, p. 225–253.
[114] Mathiesen BV, Rijhan I, Connolly D, Nielsen MP, Hendriksen PV, Mogensen MB. et al. Technology data for high temperature solid oxide electrolyser cells, alkali and PEM electrolysers; 2013.
[115] Schnurnberger W, Janßen H, Wittstadt U. Wasserspaltung mit Strom und Wärme. FVS Theme 2004:50–9.
[116] Suermann M, Schmidt TJ, Buchi FN. Investigation of mass transport losses in polymer electrolyte electrolysis cells. ECS Trans 2015;69(17):1141–8.
[117] Bernt M, Gasteiger HA. Influence of ionomer content in IrO 2 /TiO 2 electrodes on PEM water electrolyzer performance. J Electrochem Soc 2016;163(11):F3179–89.
[118] Anderson E, Ayers K, Capuano C. R & D focus areas based on 60,000 h Life PEM water electrolysis stack experience. Freiburg; 2013.
[119] Santarelli M, Medina P, Calì M. Fitting regression model and experimental validation for a high-pressure PEM electrolyzer. Int J Hydrog Energy 2009;34(6):2519–30.
[120] Auprêtre F. Technology roadmap and lifetime expectations in PEM electrolysis. Freiburg; 2013.
[121] Cargnelli J, Evers B. Recent advances in PEM water electrolysis. Freiburg; 2013.
[122] Arico A, Siracusano S, Briguglio N, Stassi A, Alegre D, Sebastian D. et al. Electrohypem – enhanced performance and cost-effective materials for long-ter-moperation of PEM water electrolysers coupled to renewable power sources: Deliverable report; 2015.
[123] Waidhas M, Woywode P. Elektrolyse- und H2-Rückverstromungstechnik von Siemens. Leipzig; 2011.
[124] Tremel A. Electrolysis and chemical synthesis as key technologies for future power-to-product routes. München; 2014.
[125] Schiller G, Ansar A, Patz O. High temperature water electrolysis using metal supported solid oxide electrolyser cells (SOEC). Adv Sci Technol 2010;72:135–43.
[126] Brisse A, Schefold J, Zahid M. High temperature water electrolysis in solid oxide cells. Int J Hydrog Energy 2008;33(20):5375–82.
[127] Chauveau F, Mougin J, Bassat JM, Mauvy F, Grenier JC. A new anode material for solid oxide electrolyser: the neodymium nickelate Nd2NiO4+δ. J Power Sources 2010;195(3):744–9.
[128] Mougin J, Chatroux A, Couturier K, Petitjean M, Reytier M, Gousseau G, et al. High temperature steam electrolysis stack with enhanced performance and durability. Energy Procedia 2012;29:445–54.
[129] Graves C, Ebbesen SD, Mogensen M. Co-electrolysis of CO_2 and H_2O in solid oxide cells: performance and durability. Solid State Ion 2011;192(1):398–403.
[130] Zhang X, O'Brien JE, O'Brien RC, Hartvigsen JJ, Tao G, Housley GK. Improved durability of SOEC stacks for high temperature electrolysis. Int J Hydrog Energy 2013;38(1):20–8.
[131] Onda K, Kyakuno T, Hattori K, Ito K. Prediction of production power for high-pressure hydrogen by high-pressure water electrolysis. J Power Sources

2004;132(1–2):64–70.
[132] Ayers KE, Dalton LT, Anderson EB. Efficient generation of high energy density fuel from water. In: 220th ECS Meeting: ECS, 2012, p. 27–38.
[133] Momma A, Takano K, Tanaka Y, Kato T, Yamamoto A. Experimental investigation of the effect of operating pressure on the performance of SOFC and SOEC. ECS Trans 2013;57(1):699–708.
[134] Abe I, Fujimaki T, Matsubara M. Hydrogen production by high temperature, high pressure water electrolysis, results of test plant operation. Int J Hydrog Energy 1984;9(9):753–8.
[135] Dunn P, Mauterer D. High-capacity, high pressure electrolysis system with renewable power sources; 2011.
[136] van Dijk N. PEM electrolyser degradation mechanisms and practical solutions. Freiburg; 2013.
[137] Janssen H, Bringmann J, Emonts B, Schroeder V. Safety-related studies on hydrogen production in high-pressure electrolysers. Int J Hydrog Energy 2004;29(7):759–70.
[138] Schalenbach M, Carmo M, Fritz DL, Mergel J, Stolten D. Pressurized PEM water electrolysis: efficiency and gas crossover. Int J Hydrog Energy 2013;38(35):14921–33.
[139] Brengel D, Dunn P. High-capacity, high pressure electrolysis system with renewable power sources. 2012.
[140] O'Brien J, Zhang X, Housley GK, DeWall K, Moore-McAteer L, Tao G. High temperatureelectrolysis pressurized experiment design, operation, and results. INL/EXT-12-26891; 2012.
[141] Bernadet L, Gousseau G, Chatroux A, Laurencin J, Mauvy F, Reytier M. Influence of pressure on solid oxide electrolysis cells investigated by experimental and modeling approach. Int J Hydrog Energy 2015;40(38):12918–28.
[142] Siemens AG. Press release H2Future project. [February 08]; 2017. Available from: ⟨http://w5.siemens.com/web/at/de/corporate/portal/presse/presseinformationen/presse/pages/h2future.aspx⟩.
[143] Stoots CM, O'Brien JE, Herring JS, Housley GK, Milobar DG, Sohal MS. et al. Long-term degradation testing of high-temperature electrolytic cells: INL/EXT-09-16559; 2009.
[144] Stoots CM, O'Brien JE, Hartvigsen JJ Test results of high temperature steam/CO2 co-electrolysis in a 10-Cell stack: INL/CON-07-12103PREPRINT.
[145] Gahleitner G. Hydrogen from renewable electricity: an international review of power-to-gas pilot plants for stationary applications. Int J Hydrog Energy 2013;38(5):2039–61.
[146] Bailera M, Lisbona P, Romeo LM, Espatolero S. Power to Gas projects review: lab, pilot and demo plants for storing renewable energy and CO_2. Renew Sustain Energy Rev 2017;69:292–312.
[147] Sigurbjörnsson OF. Sustainable fuels and chemicals by carbon recycling; 13; 2015.
[148] Sunfire GmbH. Webpage. [December 19]; 2016. Available from: ⟨http://www.sunfire.de/de/⟩.
[149] Anderson E. Advancement in PEM electrolysis & the realization of MW scale. Hannover, Germany; 2015.
[150] Schiller M, Anderson E. Five considerations for large-scale hydrogen electrolyzer development. Gas Energy 2014;1:44–7.
[151] Udagawa J, Aguiar P, Brandon N. Hydrogen production through steam electrolysis: control strategies for a cathode-supported intermediate temperature solid oxide electrolysis cell. J Power Sources 2008;180(1):354–64.
[152] Harrison K. Renewable electrolysis integrated systems development and testing; 2012.
[153] Thüga Aktiengesellschaft. Project webpage Strom zu Gas Demonstrationsanlage. [January 12]; 2017. Available from: ⟨http://www.szg-energiespeicher.de/⟩.
[154] Reissner R, Vaes J, Hosseiny SS. RESelyser: System Concept for a combined RES-Electrolyser plant with optimised efficiency: Part 2 Modern electrolyser systems and aspects of connecting to Renewable Energy sources. [January 04]; 2017. Available from: ⟨http://www.reselyser.eu/⟩.
[155] Müller-Syring G, Henel M, Köppel W, Mlaker H, Sterner M, Höcher T. et al. Entwicklung von modularen Konzepten zur Erzeugung, Speicherung und Einspeisung von Wasserstoff und Methan ins Erdgasnetz: Abschlussbericht DVGW-Projekt G1-07-10; 2013.
[156] Barisic M. Alkaline electrolysis at ELB Elektrolysetechnik GmbH. Telephone communication; 2013.
[157] Otten R. Audi e-fuels: energy carriers based on CO_2. Berlin, Germany; 2015.
[158] Petipas F, Fu Q, Brisse A, Bouallou C. Transient operation of a solid oxide electrolysis cell. Int J Hydrog Energy 2013;38(7):2957–64.
[159] Emonts B. Weltweit größtes Photovoltaik-Wasserstoff-Komplettsystem: Phoebus - solare Wasserstoff-Erzeugung. HZwei – das Magazin für Wasserstoff und Brennstoffzellen;4; 2001.
[160] Bergen A, Pitt L, Rowe A, Wild P, Djilali N. Transient electrolyser response in a renewable-regenerative energy system. Int J Hydrog Energy 2009;34(1):64–70.
[161] James B, DeSantis D, Moton J, Saur G Current hydrogen production from central solid oxide electrolysis; Available from: ⟨http://www.hydrogen.energy.gov/h2a_production.html⟩.
[162] Felgenhauer M, Hamacher T. State-of-the-art of commercial electrolyzers and on-site hydrogen generation for logistic vehicles in South Carolina. Int J Hydrog Energy 2015;40(5):2084–90.
[163] Delplancke J-L. FCH 2 JU funded water electrolysis projects – status and perspectives. Freiburg, Germany; 2016.
[164] Richter A, Pedersen CF, Mogensen M, Jensen S, Sloth M, Chen M. et al. planSOEC – R & D and commercialization roadmap for SOEC electrolysis, R & D of SOEC stacks with improved durability: Project report; 2011.
[165] ITM Power. The development of a PEM electrolyzer AST; 2014.
[166] Rakousky C, Reimer U, Wippermann K, Kuhri S, Carmo M, Lueke W, et al. Polymer electrolyte membrane water electrolysis: restraining degradation in the presence of fluctuating power. J Power Sources 2017;342:38–47.
[167] Anderson E. Cost reduction strategies for PEM electrolysis. Herten, Germany; 2015.
[168] Peterson D, Miller E Hydrogen production cost from solid oxide electrolysis: DOE hydrogen and fuel cells program record 16014.
[169] Ainscough C, Peterson D, Miller E Hydrogen production cost from PEM electrolysis: DOE hydrogen and fuel cells program record 14004; 2014.